PREDICTION OF CUTTING FORCE IN END-MILLING OPERATION OF MODIFIED AISI P20 TOOL STEEL

MUHAMAD NAZUMI BIN BASUKI

BACHELOR OF ENGINEERING
UNIVERSITI MALAYSIA PAHANG

UNIVERSITI MALAYSIA PAHANG

FACULTY OF MECHANICAL ENGINEERING

We certify that the project entitled "*Prediction of Cutting Force in End-Milling Operation of Modified AISI P20 Tool Steel*" is written by *Muhamad Nazumi Bin Basuki*. We have examined the final copy of this project and in our opinion; it is fully adequate in terms of scope and quality for the award of the degree of Bachelor of Engineering. We herewith recommend that it be accepted in partial fulfillment of the requirements for the degree of Bachelor of Mechanical Engineering with Manufacturing Engineering.

....

Encik Ramli Junid

PREDICTION OF CUTTING FORCE IN END-MILLING OPERATION OF MODIFIED AISI P20 TOOL STEEL

MUHAMAD NAZUMI BIN BASUKI

A report submitted in partial fulfillment of
The requirements for the award of the degree of
Bachelor of Mechanical Engineering
With Manufacturing Engineering

Faculty of Mechanical Engineering
UNIVERSITI MALAYSIA PAHANG

NOVEMBER 2009

SUPERVISOR'S DECLARATION

I hereby declare that I have checked this project and in my opinion, this project is adequate in terms of scope and quality for the award of the degree of Bachelor of Mechanical Engineering with Manufacturing Engineering.

Signature : ....

Name of Supervisor : DR. KUMARAN A/L KADIRGAMA

Position : LECTURER OF FACULTY MECHANICAL ENGINEERING

Date : ....

STUDENT'S DECLARATION

I hereby declare that the work in this project is my own except for quotations and summaries which have been duly acknowledged. The project has not been accepted for any degree and is not concurently submitted for award of other degree.

Signature : ....
Name : MUHAMAD NAZUMI BIN BASUKI
ID Number : ME 06063
Date : ....

To my Beloved Family and Friends:

ENCIK BASUKI BIN AHMAD

PUAN JARDINAH BINTI MAHMUD

MOHD NORIEMAN BIN BASUKI

ROSHAMIZA BINTI ROSLAN

CADENCE ISIS TAY

MOHD YAZID BIN ABU

ACKNOWLEDGEMENTS

I would like to acknowledge and extend our heartfelt gratitude to my supervisor Dr. Kumaran a/l Kadirgama; Lecturer of Faculty Mechanical Engineering for his continues support, helpful advice and valuable guidance throughout my thesis. This thesis could not have been done without Dr. Kumaran who not only served as my supervisor but also encouraged and guide me through the writing up thesis process by giving his best effort. I also wish to express my sincere appreciate to the lecturers, technical staffs of Faculty Mechanical Engineering, University Malaysia Pahang for their teaching and help during the period of the project.

I also wish to express sincere appreciation to all my friends for their advice to do the study. I benefited greatly from the comments and wisdom these reviewers generously shared with me.

I acknowledge my sincere indebtedness and gratitude to my parents, Encik Basuki bin Ahmad and Puan Jardinah binti Mahmud for their love, dream and sacrifice throughout my life. They have always sacrifices their time and continuous support me to achieve my dreams and goals. I would like to thank them for all support and encouragement they done for me. Besides that I also want to express my appreciation to my younger brother Mohd Norieman bin Basuki and my friend, Mohd Yazid bin Abu for giving their idea, support, and help throughout this project. I truly could not have done my thesis without them.

ABSTRACT

This thesis discuss the development of the first and second order models for predicting the cutting force produced in end-milling operation of modified AISI P20 tool steel. The first and second order cutting force equations are developed using the response surface methodology (RSM) to study the effect of four input cutting parameters which is cutting speed, feed rate, radial depth and axial depth of cut on cutting force. The cutting force contours with respect to input parameters are presented and the predictive models analyses are performed with the aid of the statistical software package Minitab. The separate affect of individual input factors and the interaction between these factors are also investigated in this study. In first order model, the decrease of cutting speed along with the increase in the cutting speed, feed rate, axial and radial depths of cut will cause the cutting force to become larger. The received second order equation shows, based on the variance analysis, that the cutting force increased when federate and radial depth of cut is raised. However, the cutting force increased with the slightly reduce of axial depth and cutting speed value. The predictive models in this study are believed to produce values of the longitudinal component of the cutting power close to those readings recorded experimentally with a 95% confident interval.

ABSTRAK

Kertas tesis ini membincangkan perkembangan dalam pertama dan kedua susunan model untuk menjangkakan daya pemotongan yang dihasilkan dalam operasi hujung kisaran terhadap modifikasi AISI P20 alatan besi. Persamaan pertama dan kedua susunan daya pemotongan telah dikembangkan dengan menggunakan kaedah tindakbalas permukaan untuk mempelajari kesan terhadap empat pengeluar daya pemotongan di mana ianya adalah kelajuan pemotongan, kadar pembekal, kedalaman axial dan radial terhadap daya pemotongan. Kecerunan daya pemotongan yang berkait dengan parameter pengeluar telah dibentangkan dan jangkaan model yang dianalisis telah dilakukan dengan bantuan perisian statistik Minitab. Pembahagian kesan terhadap individu faktor pengeluar dan interaksi antara factor-faktor ini juga telah disiasat dalam kertas tesis ini. Dalam susunan model pertama, penurunan kelajuan pemotongan seiring dengan peningkatan kadar pembekal, kedalaman axial dan radial terhadap daya pemotongan telah menyebabkan daya pomotongan juga meningkat. Penerimaan persamaan susunan kedua berdasarkan perbezaan analisis di mana daya pemotongan bertambah apabila kadar pembekal dan radial terhadap kekuatan pemotongan telah dinaikkan. Namun, peningkatan daya pemotongan berlaku dengan sedikit penurunan nilai kedalaman axial dan kelajuan pemotongan. Jangkaan model dalam kertas tesis ini dipercayai dapat menghasilkan nilai komponen membujur terhadap daya pemotongan menghampiri kepada bacaan yg direkodkan secara experimen dengan 95% jeda keyakinan.

TABLE OF CONTENTS

LIST OF TABLES

LIST OF FIGURES

LIST OF SYMBOLS

Vc	Velocity vector
kC	Specific cutting force
FD	Thrust force
F	Cutting power response
cs	Cutting speed
fr	Federate
ad	Axial depth
rd	Radial depth
y	Cutting power experimental value
$\hat{y}$	Cutting power predicted value
β_0, β_1, β_2, β_3 and β_4	Model parameter
ε	Experimental error
Fy	Force component
x_0	Dummy variable
x_1, x_2, x_3 and x_4	Cutting speed, feed rate, axial depth of cut and radial depth of cut substitute in cutting force model.

LIST OF ABBREVIATIONS

AISI	American Iron Steel Institute
ANOVA	Analysis of Variance
ASME	American Society Mechanical Engineer
BUE	Built Up Edge
CAD	Computer Aided Design
CAM	Computer Aided Manufacturing
CVD	Chemical Vapor Deposition
CNC	Computer Numerical Control
DOE	Design of Experiment
HSS	High Speed Steel
ISO	International Standard Organization
NN	Neural Network
PVD	Physical Vapor Deposition
RSM	Response Surface Methodology

UNIVERSITI MALAYSIA PAHANG

BORANG PENGESAHAN STATUS TESIS♦

JUDUL: **PREDICTION OF CUTTING FORCE IN END-MILLING OPERATION OF MODIFIED AISI P20 TOOL STEEL**

SESI PENGAJIAN: **2009/2010**

Saya **MUHAMAD NAZUMI BIN BASUKI (871001-02-5319)**
(HURUF BESAR)

mengaku membenarkan tesis (Sarjana Muda/~~Sarjana~~ /~~Doktor Falsafah~~)* ini disimpan di Perpustakaan dengan syarat-syarat kegunaan seperti berikut:

1. Tesis adalah hakmilik Universiti Malaysia Pahang (UMP).
2. Perpustakaan dibenarkan membuat salinan untuk tujuan pengajian sahaja.
3. Perpustakaan dibenarkan membuat salinan tesis ini sebagai bahan pertukaran antara institusi pengajian tinggi.
4. **Sila tandakan (√)

	SULIT	(Mengandungi maklumat yang berdarjah keselamatan atau kepentingan Malaysia seperti yang termaktub di dalam AKTA RAHSIA RASMI 1972)
	TERHAD	(Mengandungi maklumat TERHAD yang telah ditentukan oleh organisasi/badan di mana penyelidikan dijalankan)
√	**TIDAK TERHAD**	

Disahkan oleh:

(TANDATANGAN PENULIS) (TANDATANGAN PENYELIA)

Alamat Tetap:

9 LORONG 14, TAMAN PERUDA,
08000 SUNGAI PETANI,
KEDAH.

DR. KUMARAN A/L KADIRGAMA
(Nama Penyelia)

Tarikh: **22 NOVEMBER 2009**

Tarikh: : **22 NOVEMBER 2009**

CATATAN:
* Potong yang tidak berkenaan.
** Jika tesis ini SULIT atau TERHAD, sila lampirkan surat daripada pihak berkuasa/organisasi berkenaan dengan menyatakan sekali tempoh tesis ini perlu dikelaskan sebagai atau TERHAD.
♦ Tesis dimaksudkan sebagai tesis bagi Ijazah doktor Falsafah dan Sarjana secara Penyelidikan, atau disertasi bagi pengajian secara kerja kursus dan penyelidikan, atau Laporan Projek Sarjana Muda (PSM).

CHAPTER 1

INTRODUCTION

1.1 INTRODUCTION

The enhancement of productivity and the reliability of manufacturing systems have become more and more important in modern industry. Adequate prediction of machining performance can improve selection of correct machining conditions, save operation time and reduce waste (Won-Soo Yun and Dong-Woo Cho, 2001). An accurate model for the cutting forces is essential to analysis and prediction of machining performance. Milling operations are one of the most common machining operations in industry. It can be used for face finishing, edge finishing, material removal, etc. There are several parameters that influence the forces acting on the cutter. Because of these parameters, the forces may become unpredictable and result in larger dimensional variations when products are produced (Wen-Hsiang Lai, 2000).

As the research published by Tugrul Özel (1998), simulation of milling operations has the potential for improving cutting tool designs and selecting optimum conditions, especially in advanced applications such as machining of tool steels. This study has concentrated on developing and evaluating the mathematical models to predict surface roughness and cutting forces in a simple flat end milling operation.

The cutting force has a significant influence on the dimensional accuracy because of tool and workpiece deflection in milling. Force modeling in metal cutting is important for a multitude of purposes, including thermal analysis, tool life estimation, chatter prediction, and tool condition monitoring.

1.2 PROBLEM STATEMENT

The setting of the operational parameters range such as feed rate, rotational speed and axial depth of CNC Milling machine is the main problem face in this experiment. A good result of surface roughness and cutting force of AISI P20 tool steel are depend on the optimization of the parameters set up with aid of statistical method, using coated carbide cutting tool under various cutting conditions (Kadirgama *et al*, 2008).

1.3 OBJECTIVES

1. The objective of this study is to predict the cutting force in end-milling operation of modified AISI P20 tool steel by developing the first and second order mathematical model.
2. To investigate the relationship between cutting parameters; cutting speed, feedrate, axial depth, radial depth with cutting force.

1.4 LIMITATION

The limitation to develop the mathematical models which are the range of cutting speed is between 100 to 180 m/min, the feedrate between 0.1 to 0.2 mm/tooth, the axial depth between 1 to 2mm and the radial depth between 2 to 5mm.

1.5 OVERVIEW OF THE REPORT

Chapter 1 gives the brief the content and background of the project. The problem statement, scope of study and objectives are also discussed in this chapter.

Chapter 2 discusses about the literature review of this experiment such as CNC milling process, cutting tools, modified AISI P20 tool steel, and response surface methodology.

Chapter 3 presents the methodology and experiment setup for this project. It discuss on how the experiment be prepared with all the preparation of workpiece, experiment process and RSM.

Chapter 4 discusses the result and discussion of the project. The discussion aims is to determine the predicted cutting force at the best state of this project and the relations of the four parameters in this project.

Chapter 5 presents the conclusions of the project. Suggestions and recommendations for the future work are put forward in this chapter.

CHAPTER 2

LITERATURE REVIEW

2.1 INTRODUCTION

The purpose of this chapter is to provide a review of the past research related to the machining prospect, workpiece, cutting tool and the method to analyze the cutting force prediction of AISI P20 tool steel by using Response surface methodology (RSM). RSM is a collection of mathematical and statistical techniques that are useful for the modeling and analysis of problems in which a response of interest is influenced by several variables and the objective is to optimize this response (Montgomery, 2001).

In the manufacturing industries, various machining processes are adopted to remove the material from the work piece for a better product. Of these, the end milling process is one of the most vital and common metal cutting operations used for machining parts because of its ability to remove materials faster with a reasonably good surface quality. In recent times, Computer Numerically Controlled (CNC) machine tools have been implemented to realize full automation in milling since they provide greater improvements in productivity increase the quality of the machined parts and require less operator input.

2.2 CNC MILLING

CNC stands for “Computer Numeric Control” which is how a computer talks to a milling machine to control its movements to cut the part you design. The language it uses is called “G-code”, which is a series of instructions that, combined with X, Y and Z coordinates denotes direction, speeds and key points of the shape to be cut. In the past, for example, even the most skilled machinist would have a problem cutting a circle because both the X and Y handwheels would have to be cranked at the same time at constantly varying rates at the same time. The computer, however, has no trouble doing this, and a complicated shape can be cut just as easily as a straight line. The advantage of CNC beyond cutting difficult 3D shapes is that once the program is written and the holding fixtures made, multiple identical parts can be made rapidly (sherline.com).

Recent developments in manufacturing industry have contributed to increase the importance of computerized numerical control milling operations. Milling process is one of the most popular and effective machining operations. Computer Numerical Control (CNC) Milling is the most common form of CNC. CNC mills can perform the functions of drilling and often turning. CNC Mills are classified according to the number of axes that they possess. Axes are labeled as x and y for horizontal movement, and z for vertical movement.

2.2.1 Cartesian Coordinate System

The basis for all machine movement is the Cartesian coordinate system (Fig. 2.1). Programs in either inch or metric units specify the destination of a particular movement. With it, the axis of movement (X, Y, or Z) and the direction of movement (+ or –) can be identified. Some machining centers may have as many as five or six axes, but for our purposes we will only discuss three axes. To determine whether the movement is positive (+) or negative (–), the program is written as though the tool, rather than the work, is doing the moving (NAVY-repairmans-manual-Chapter11).

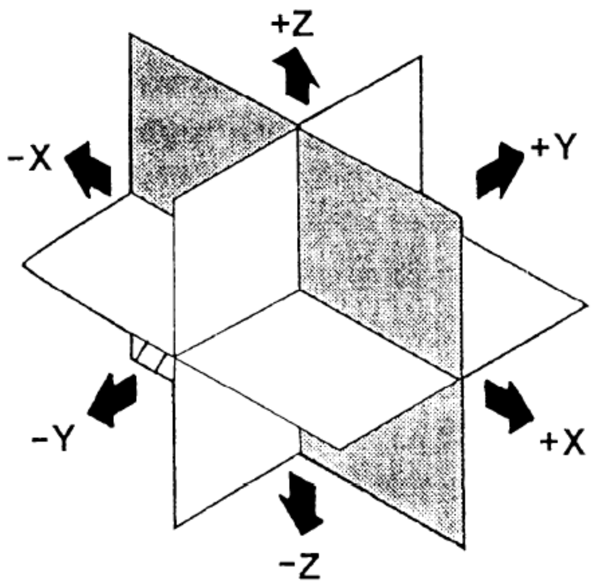

Figure 2.1: Cartesian coordinate system

Source: NAVY-repairmans-manual-Chapter11

Spindle motion is assigned the Z axis. This means that for a drill press or vertical milling machine the Z axis is vertical, as shown in Figure 2.2. For machines such as lathes or horizontal milling machines, the Z axis is horizontal (NAVY-repairmans-manual-Chapter11).

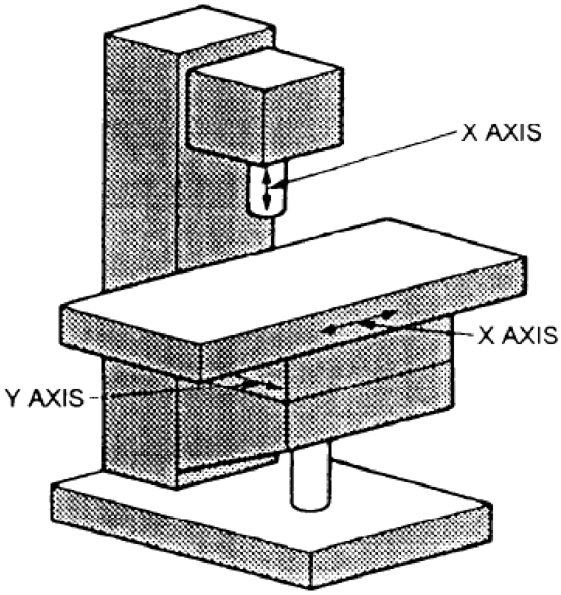

Figure 2.2: Three-axis vertical mill.

Source: NAVY-repairmans-manual-Chapter11

2.2.2 End Milling

The end milling cutter can be divided into a finite number of disk elements and the total *x*-, *y*-, and *z*-force components acting on a flute at a particular instant are obtained by numerically integrating the force components acting on an individual disk element. Finally, a summation over all flutes engaged in cutting yields the total forces acting on the cutter at that time. Fig. 2.3 shows schematic views of an end milling process geometry and coordinate system.

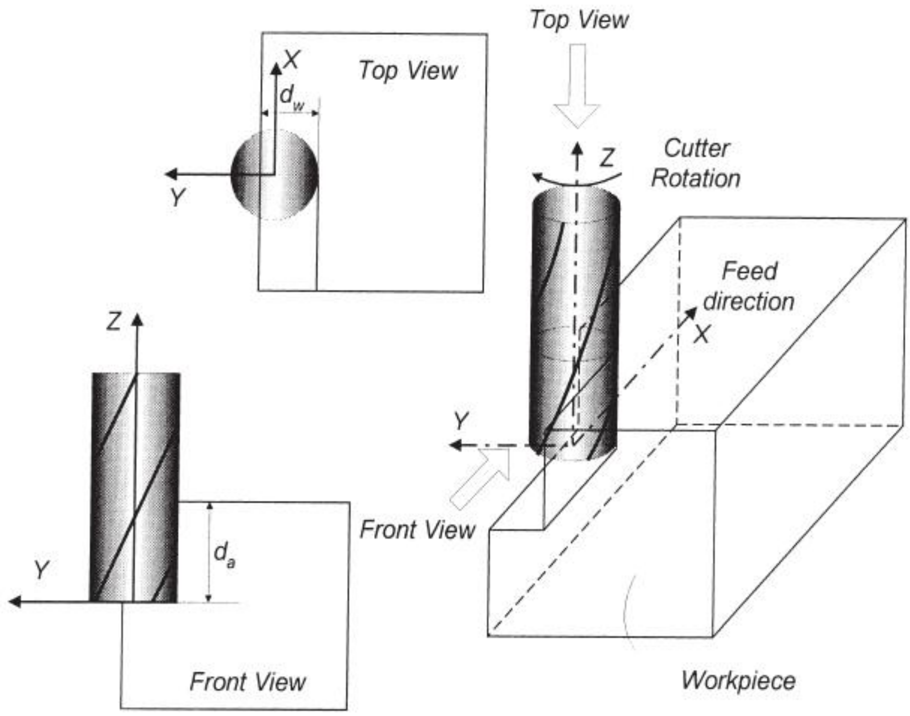

Figure 2.3: Schematic views of the basic end milling process geometry and coordinate.

Source: Won-Soo Yun and Dong-Woo Cho (2001)

2.3 MODIFIED AISI P20 TOOL STEEL

AISI P20 is mold quality alloy steel supplied in the prehardened condition. Special melting and refining practices are utilized to produce a uniform product with exceptional cleanliness. These characteristics allow AISI P20 to be polished to an extremely high finish required for plastic molding. The material is tested to rigorous tool steel standards to ensure uniformity of structure and freedom from defects. AISI P20 is supplied prehardened to 262/321 BHN. The balanced alloy composition of AISI P20 ensures a uniform cross-sectional hardness (diehlsteel). Table 2.1 shows the guideline for machining AISI P20 material for turning and milling operation according to the suitable range of parameters.

Table 2.1: Guideline for machining for turning and milling operation

Turning Carbide Tools	Rough Turning	Medium Turning	Finish Turning
Depth of cut (t) mm	min. 10	2-10	max. 2
Feed (s) mm.p.r.	mm 1.0	0.3-1.0	max. 0.3
ISO Machining Group	P30-P40	P20-P30	P10
Cutting Speed (v) m/min	40-60	60-100	90-160
Milling Carbide Tools & High Speed Steel Tools		**Rough Milling**	**Finish Milling**
Depth of cut (t)		min. 2	max. 2
Feed (s) mm/tooth		min. 0.2	max. 0.2
ISO Machining Group		P30-P40	P10-P20
Cutting Speed (v) m/min. (Carbide Tools)		55-85	75-95
Cutting Speed (v) m/min. (High Speed Steel Tools)		10-20	15-30

Source: Westyorkssteel.com

2.3.1 Composition and Typical Properties

Generally, AISI P20 is a chromium-molybdenum alloyed steel which is considered as a high speed steel used to build moulds for plastic injection and zinc die-casting, extrusion dies, blow moulds, forming tools and other structural components. The modified form of AISI P20 is distinguished from normal P20 steel by the balanced sulphur content (0.015%) which gives the steel better machinability and more uniform hardness in all dimensions. Modified AISI P20 possesses a tensile strength of 1044 MPa at room temperature and a hardness ranging from 280 to

320 HB. The workpiece used in this study was prehardened and tempered to a minimum hardness of 300 HB and was provided by ASSAB (Sweden) (K. Kadirgama, *et.al* 2008). The approximate chemical analysis is shown in Table 2.2.

Table 2.2: Typical composition of Modified AISI P20

Composition	Percentage
C	0.38
Si	0.3
Mn	1.5
Cr	1.9
Mo	0.15
S	0.015
Fe	Balance

Source: K. Kadirgama, *et.al* (2008)

By definition, steel is a combination of iron and carbon. Steel is alloyed with various elements to improve physical properties and to produce special properties such as resistance to corrosion or heat. Specific effects of the addition of such elements are outlined below (diehlsteel):

- Carbon (C) is the most important constituent of steel. It raises tensile strength, hardness, and resistance to wear and abrasion. It lowers ductility, toughness and machinability.
- Silicon (Si) is a deoxidizer and degasifier. It increases tensile and yield strength, hardness, forgeability and magnetic permeability.
- Manganese (Mn) is a deoxidizer and degasifier and reacts with sulfur to improve forgeability. It increases tensile strength, hardness, hardenability and resistance to wear. It decreases tendency toward scaling and distortion. It increases the rate of carbon-penetration in carburizing.
- Chromium (Cr) increases tensile strength, hardness, hardenability, toughness, resistance to wear and abrasion, resistance to corrosion, and scaling at elevated temperatures.

- Molybdenum (Mo) increases strength, hardness, hardenability, and toughness, as well as creep resistance and strength at elevated temperatures. It improves machinability and resistance to corrosion and it intensifies the effects of other alloying elements. In hot-work steels and high speed steels, it increases red-hardness.
- Sulfur (S) improves machinability in free-cutting steels, but without sufficient manganese it produces brittleness at red heat. It decreases weldability, impact toughness and ductility.

P20 is a pre hardened high tensile tool steel which offers ready machineability in the hardened and tempered condition, therefore does not require further heat treatment . This eliminates the risks, cost, and waiting time of heat treatment thus avoiding the associated possibility of distortion or even cracking. Subsequent component modifications can easily be carried out.

There are some technical data that we should know according to AISI P20 characteristics. In forging this material, heat slowly and uniformly to 1050°C, Do not forge below 930°C and after forging cool slowly. In annealing, P20 should always be annealed after forging and before rehardening. It must be heat uniformly to 770/790°C and after that soak well and cool slowly in the furnace. In case of hardening**,** heat uniformly to 820/840°C until heated through and quench in oil. Besides that, tempering need to heat uniformly and thoroughly at the selected tempering temperatures and hold for at least one hour per inch of total thickness. All this explanation can conclude in this Thermal Cycle Diagram as in Figure 2.4.

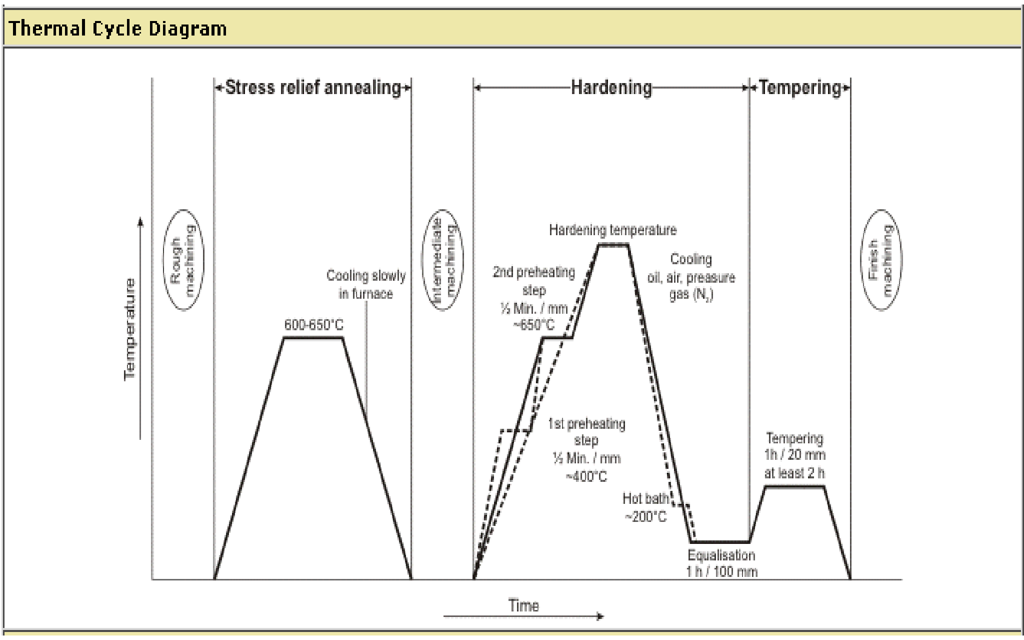

Figure 2.4: Thermal Cycle Diagram of P20 tool steel

For nitriding, moulds machined from pre hardened P20 may be nitrided to give a hard surface which is very resistant to wear and erosion. A nitrided surface also increases the corrosion resistance. The surface hardness after nitriding at a temperature of 525° C in ammonia gas will be approximately 650HV. Moreover, tufftriding at 570° C will give a surface hardness of approximately 700HV. After hours treatment the hard layer will be approximately 0.01mm. In flame and induction hardening, P20 can be flame or induction hardened to a hardness of 50 to 55 HRC and cooling in air is preferable. Smaller pieces may however require forced cooling and hardening should be immediately followed by tempering. In addition, in welding process heat to approximately 400 to 500° C. Weld at approximately 400 to 500° C and stress relieve. Use Chromium-Nickel-Molybdenum-alloyed basic electrodes for welding of structural steels. Welding may also be carried out using an austenitic stainless steel electrode. In this case the stipulated increased working temperature may be modified, but the weld metal has a lower strength than the parent material. Table 2.3 shows the physical properties of P20 tool steel.

Table 2.3: Physical properties of P20 tool steel

USA: **AISI P20**		
Chemical composition: C=0.4%, Mn=1.5%, Si=0.4%, Cr=1.9%, Mo=0.2%		
Property	**Value in metric unit**	
Density	$7.81 * 10^3$	kg/m³
Modulus of elasticity	205	GPa
Thermal expansion (20 ºC)	$12.8 * 10^6$	$ºC^{-1}$
Specific heat capacity	460	J/(kg*K)
Thermal conductivity	29	W/(m*K)
Annealing temperature	850...900	ºC
Quenching temperature	860...880	ºC
Tempering temperature	200...590	ºC
Hardness (annealed)	95	RB
Hardness (hardened)	52	RC
Quenching medium	Oil	

Source: Substech.com

2.4 CUTTING FORCES

The cutting forces during machining operations are often predicted from empirical equations. The required constants or parameters for these equations are determined experimentally. These techniques are useful and necessary, but the resulting equations and parameters are often limited to the particular operation and conditions tested. In die and mold machining, where the cutting conditions vary widely, a prohibitive amount of test cuts may be needed to determine the parameters (Won-Soo Yun and Dong-Woo Cho, 2001).

Figure 2.5 shows the relationship between the resultant cutting forces and cutting speeds measured under various machining environments. As expected, the resultant cutting force was the highest under dry cutting conditions. The higher cutting forces were due to the effect of adhesion of the work material on the tool. The cutting forces were lower when the tool was sharp during the initial stages of machining and was seen to increase as adhesion on the tool progresses. The resultant force was seen to be the lowest with flooded coolant system (P.S. Sreejith**,** 2008).

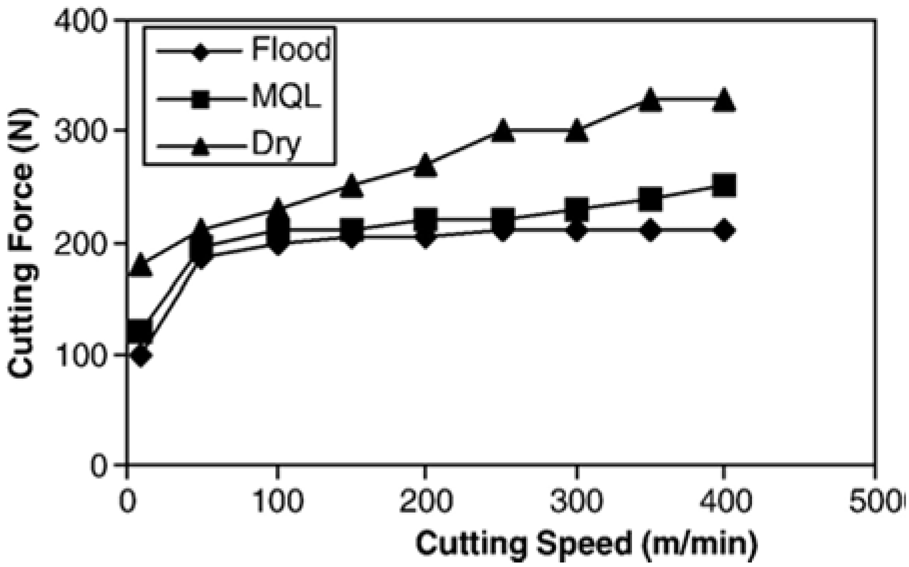

Figure 2.5: Resultant cutting forces and cutting speeds measured under various machining environments

Source: P.S. Sreejith **(**2008)

This is because due to the flooded cooling, the adhesion on the tool is lowest. This lower adhesion produces lower frictional force. MQL machining also reduces the frictional forces like flooded conditions, but for getting a lower resultant force like flooded system, a further investigation on the constituents of the coolant has to be carried out.

2.5 RESPONSE SURFACE METHOD (RSM)

The response surface method (RSM) is practical, economical and relatively easy for use. The experimental data was utilized to build mathematical model for first- and second-order model, by regression method. This method has been used by some researchers for tool life and surface roughness **(**Yusuf Sahin**,** 2004). In order to eliminate or reduce cracks and porosity, response surface methodology (RSM) was used to understand the relationship between laser processing parameters and the defects (cracks and porosity) (V.E. Beal, 2006). RSM is utilized to create an efficient analytical model for surface roughness in terms of cutting parameters: feed, cutting speed, axial depth of cut, radial depth of cut and machining tolerance (H. Öktem**,** 2005).

The RSM technique attains convergence by repeating numerical and sensitivity analysis until the optimal solution as obtained. For problems with high non-linearity, and for multimodal problems, there may be cases in which no solution can be found because of problems such as inability to obtain sensitivities or a lapse into a local solution. To solve such problems with conventional optimization, the RSM has been adopted. With RSM, optimization conditions are first set, and then a response surface is created between design variables and objective functions or constraint conditions (Amago**).** Since the expected experimental and theoretical relations in machining are expected to be non-linear, in this work response surface models are used for optimization.

The mathematical model generally used is represented by Eq. (2.1)

$$Y = f\,(v, f, \alpha, r) + € \tag{2.1}$$

where Y is the machining surface response, v, f, α, r are milling variables, and € is the error which is normally distributed about the observed response Y with zero mean. Considering only the parameters v and f, a relation can be formulated between these independent variables and the dependent variable, surface roughness Ra, as Eq. (2.2) (Alauddin *et al*, 1996)

$$R_a = C v^a f^b \tag{2.2}$$

where C is a constant, v is cutting speed (m/min), f is the feed rate (mm/min), and a and b are the empirically-estimated exponents. This mathematical model is linearized by performing a logarithmic transformation as Eq. (2.3)

$$\ln R_a = \ln C + a \ln v + b \ln f \tag{2.3}$$

The constants and exponents C, a, and b can be determined by the method of least squares. The first order linear model, developed from the above functional relationship using the least square method, can be represented as Eq. (2.4)

$$Y_1 = Y - \in = b_0x_0 + b_1x_1 + b_2x_2 \quad (2.4)$$

where Y1 is the estimated response. Based on the first-order equation, Y is the measured surface roughness on a logarithmic scale, x0(=1) is a dummy variable; x1 and x2 are logarithmic transformations of cutting speed and feed. b0, b1 and b2 are coefficients found from least squares method (Kurt and Andrew Otieno, 2008).

The RSM is a set of techniques that encompasses (Montgomery and Peck, 1992),

- The designing of a set of experiments for adequate and reliable measurement of the true mean response of interest
- The development of mathematical model with best fits
- Finding the optimum set of experimental factors that produces maximum or minimum value of response
- Representing the direct and interactive effects of process variables and surface roughness through two dimensional graphs.
- The adequacy of the model has been checked through *F*-test and plotting scatter diagram.

The average cutting forces are determined at different feed rates in tangential, radial, and axial directions per tooth period by keeping immersion and axial depth of cut as constant. A comparison between modeling and experiment is presented. This model and analysis are useful not only for predicting the tool wear but also for selecting optimum process parameters for achieving the stability of the end milling process. Nevertheless, response surface methodology developed mathematical models for surface roughness in order to optimize the surface finish of the machined surface

(Mansour, A. and Abdalla, H. 2002; El baradie, M. A. 1993; K. A. Rosentrater, A. Otieno and P. Melampati. 2008).

2.6 FORCE MEASUREMENT

Force measurement in manufacturing, especially in machining, is very important. This is because force measurement can be used for monitoring the tool conditions and avoiding breakage during the machining process. It helps us understand machining process, because cutting force is one of the most sensitive indicators of machining performance (Byrne *et al*, 1995). Both the static and dynamic components of the cutting force contain information concerning the state of chip formation and the cutting tool. Otherwise force measurement enables engineer to optimize manufacturing process and design proper machining tool. Since general cutting values cannot be transferred from one shop to another or from one machine to another, every manufacturer must have their own cutting data available. Some of the principle factors influencing the magnitude and direction of the cutting forces include: cutting speeds, feeds, depth of cut, stock, tool material and geometry, as well as coolant.

Cutting is the most important method of forming used in production. This is reason enough for continuous testing and optimization of this process. Even minimal savings in, for example, machining time, are very important in achieving cost effective mass production. As an example they are utilized when investigating, comparing or selecting materials, tools and machines. Further application areas emerge when determining the optimal cutting conditions, investigation of tool fracture behavior and chip formation, and their influences on cutting forces. Sensors most commonly used in such systems measure cutting force components or quantities related to cutting force (Kosmol, 1995).

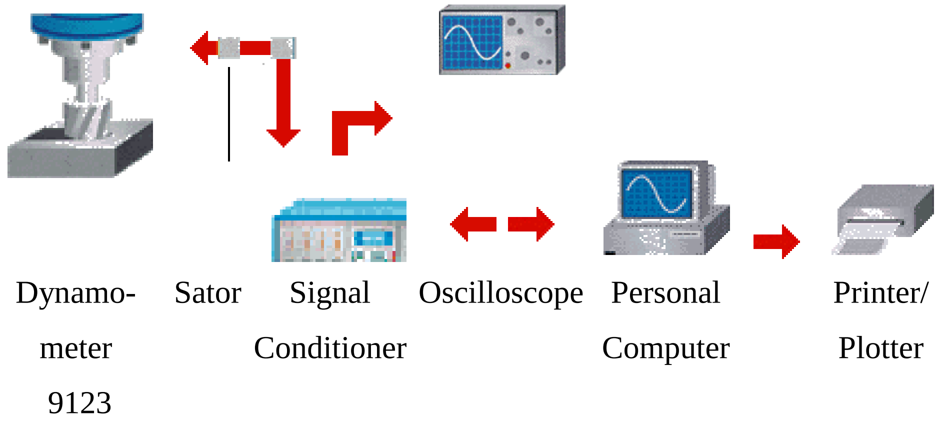

Figure 2.6: Measuring force for milling

Source: Kosmol (1995)

Force measurements were made using quartz 3–component Kistler dynometer which provides dynamic and quasi-static measurement of the three orthogonal components of a force Ff, Fr, Ft. The three charge outputs of the dynometer were converted to voltage signals using the Kistler dual mode charge amplifiers and the graphs of the cutting force were obtained by using the dynoware software in the computer that illustrated by the figure 2.6.

Force measurements in the cutting, radial and feed directions for 25 tests are observed by P. Thangavel and V. Selladurai (2008), using dynometer. The sensitivity of the cutting force or tangential force, Ft to progressive wear is observed to be much higher than that of the radial, Fr and Feed, Ff forces that are shown in Figures 2.7 (a) and (b).

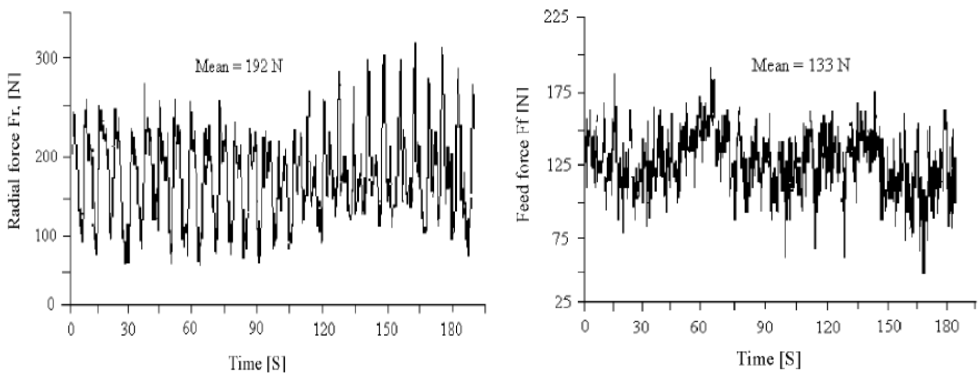

(a) Graph of radial force and feed force

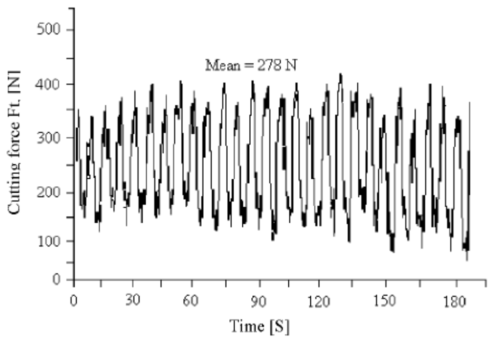

(b) Graph of cutting force

Figure 2.7: Grapf shows in the dynoware: (a) Graph of radial force and feed force show in the dynoware and; (b) Graph of cutting force shows in the dynoware

Source: P. Thangavel and V. Selladurai (2008)

2.7 COOLANT / LUBRICANT

The cooling applications in machining operations play a very important role and many operations cannot be carried out efficiently without cooling. Application of a coolant in a cutting process can increase tool life and dimensional accuracy, decrease cutting temperatures, surface roughness and the amount of power consumed in a metal cutting process and thus improve the productivity (Yakup Yildiz, Muammer Nalbant, 2008).

The effect of dry machining, minimum quantity of lubricant (MQL), and flooded coolant conditions was analyzed with respect to the cutting forces, surface roughness of the machined work-piece and tool wear. The three types of coolant environments are the other problems facing in this project (P.S. Sreejith**,** 31 January 2008). To find a good surface finish of this soft material, the quantity and the type of coolant are important factors to optimize the result. It is found that MQL condition will be a very good alternative to flooded coolant/lubricant conditions. Therefore, it appears that if MQL properly employed can replace the flooded coolant/lubricant environment which is presently employed in most of the cutting/machining applications, thereby not only the machining will be environmental friendly but also will improve the machinability characteristics.

The cooling applications in machining operations play a very important role and many operations cannot be carried out efficiently without cooling. Application of a coolant in a cutting process can increase tool life and dimensional accuracy, decrease cutting temperatures, surface roughness and the amount of power consumed in a metal cutting process and thus improve the productivity (P.Sahoo *et al*, 2008).

As a study from P.S. Sreejith (31 January 2008), many of the fluids, which are used to lubricate metal forming and machining, contain environmentally harmful or potentially damaging chemical constituents. These fluids are difficult to dispose and expensive to recycle and can cause skin and lung disease to the operators and air pollution. Without the cooling effects of fluid, a metalcutting process may produce excessive heat that subjects the workpiece material to high stress and the danger of thermal expansion (Christina Dunlap, 1997).

2.7.1 Types of Coolant

Conventional cutting fluids were classified into three groups as seen in Fig. 2.8 (Baradie, 1996). Water soluble fluids were defined suitable for operations where cutting speeds were very high and pressures on the tool were relatively low. Neat cutting oils are straight mineral oils, or mineral oils with additives. They were preferred when cutting pressures between chip and tool face were very high and where the primary consideration was lubrication. It was determined that cutting fluids cannot penetrate the chip–tool interface at high-cutting speeds by M.C. Shaw. Gaseous lubricants were seen very attractive when the cutting fluid penetration problem was considered but the high cost of gases made them uneconomical for production applications.

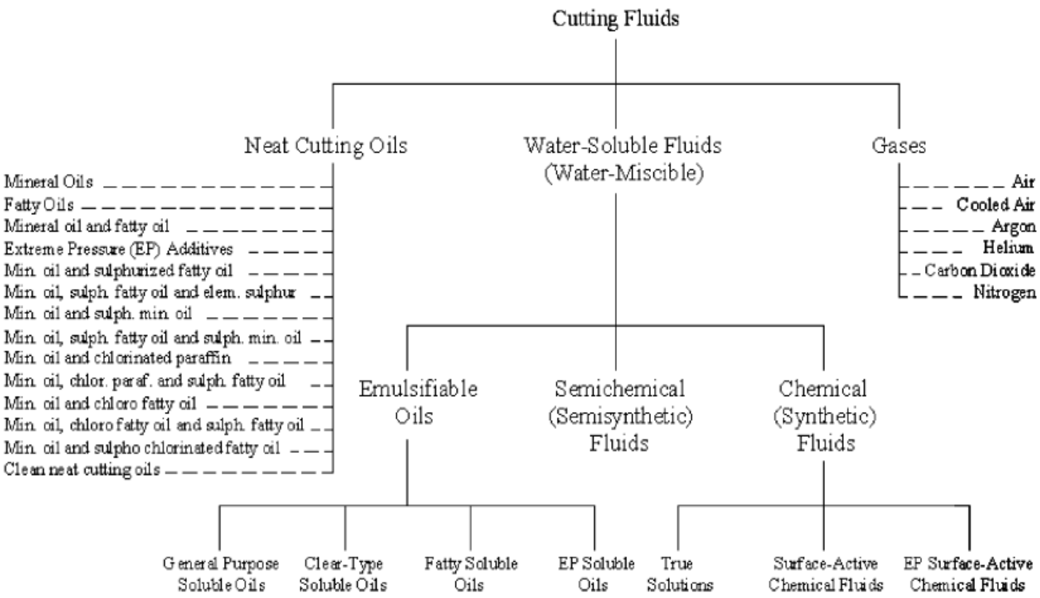

Figure 2.8: Classification of cutting fluids

Source: Baradie (1996).

2.8 CUTTING TOOL

There are many different tool-holding devices used for CNC machines. They can be as simple as a quick-change tool post or as complicated as an automatic tool change system, but they all serve the same purpose. The tool-holding devices for each shop will vary since each machine comes with different tooling and because shop personnel will purchase the tooling they prefer. Cutting tools are available in three basic material types: high-speed steel, tungsten carbide, and ceramic.

Coated carbide tools are known to perform better than uncoated carbide tools. Two-thirds of all carbide tools are coated. Coated tools should be considered for most applications because of their longer life and faster machining. Coating broadens the applications of a specific carbide tool. These coatings are applied in multiple layers of under .001 of an inch thickness. The main carbide insert and cutting tool coating materials are titanium carbide, titanium nitride, aluminum oxide, and titanium carbonitride and these are approve by the society of manufacturing engineers.

Although a material may not be hard, elements and processes added during production may aid in the breakdown of cutting edges or forming lobes. In surface lubricity, a high coefficient of friction causes increased heat, leading to a shorter coating life or coating failure. However, a lower coefficient of friction can greatly increase tool life. The amount of heat can be reduced by a surface that lacks coarseness or irregularities. This slick surface lets the chips slide off the face of the tool, generating less heat. A higher surface lubricity also can allow for increased speeds when compared to non-coated versions (Scott, 2009). Figure 2.9 shows the TiN insert coated carbide cutting tools used in this study that is a general purpose PVD coating that increases hardness and has a high oxidation temperature. This coating works great while cutting or forming with HSS tooling.

Figure 2.9: TiN insert coated carbide attached to the tool holder 2-flute

A higher oxidation temperature rating improves success in high heat applications. Although the Titanium Aluminum Nitride (TiAlN) coatings may not be as hard as TiCN at room temperature, it proves to be much more effective in applications where heat is generated. This coating holds its hardness at higher temperatures due to a layer of aluminum oxide that forms between the tool and the cutting chip. This layer transfers heat away from the tool and into the part or chip. Carbide tooling is generally run at higher speeds compared to high speed steel. This makes TiAlN a preferred choice when coating carbide. Drills and end mills are commonly coated with this type of physical vapor deposition treatment. In anti-seizure, this property keeps material from depositing onto the tool by preventing less chemical reactivity between the tool and the cutting material.

CHAPTER 3

METHODOLOGY

3.1 INTRODUCTION

This chapter presents the overall methodology of this project that includes specifications of every tools that used in this project and the procedures to run the MINITAB software.

3.2 WORKPIECE

Generally, AISI P20 is a chromium-molybdenum alloyed steel which is considered as a high speed steel used to build moulds for plastic injection and zinc die-casting, extrusion dies, blow moulds, forming tools and other structural components. The modified form of AISI P20 is distinguished from normal P20 steel by the balanced sulphur content (0.015%) which gives the steel better machinability and more uniform hardness in all dimensions. Modified AISI P20 possesses a tensile strength of 1044 MPa at room temperature and a hardness ranging from 280 to 320 HB. The workpiece used in this study was prehardened and tempered to a minimum hardness of 300 HB and was provided by ASSAB (Sweden) (K. Kadirgama, *et.al* 2008). Applications for AISI P20 tool steel are plastic moulds, frames for plastic pressure dies, hydroforming tools. The approximate chemical analysis is shown in Table 3.1.

Table 3.1: Typical composition of Modified AISI P20

Composition	Percentage
C	0.38
Si	0.3
Mn	1.5

Cr	1.9
Mo	0.15
S	0.015
Fe	Balance

Source: K. Kadirgama, *et.al* (2008)

Table 2.2 shows the physical properties of P20 tool steel and Figure 3.1 below shows the specific dimension of AISI P20 tool steel which is 100mm×170mm×25.4mm.

Table 3.2: Physical properties of P20 tool steel

***USA*: AISI P20**		
Chemical composition: C=0.4%, Mn=1.5%, Si=0.4%, Cr=1.9%, Mo=0.2%		
Property	**Value in metric unit**	
Density	$7.81 * 10^3$	kg/m^3
Modulus of elasticity	205	GPa
Thermal expansion (20 ºC)	$12.8 * 10^6$	$ºC^{-1}$
Specific heat capacity	460	J/(kg*K)
Thermal conductivity	29	W/(m*K)
Annealing temperature	850...900	ºC
Quenching temperature	860...880	ºC
Tempering temperature	200...590	ºC
Hardness (annealed)	95	RB
Hardness (hardened)	52	RC
Quenching medium	Oil	

Source: Substech.com

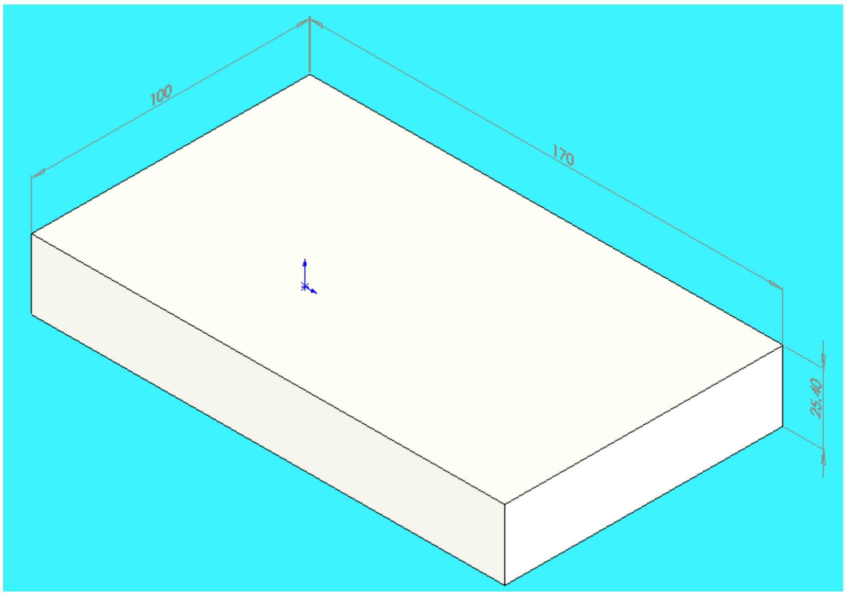

Figure 3.1: Specific dimension of AISI P20 tool steel 100mm×170mm×25.4mm

3.3 TOOLS AND EQUIPMENT

In this project, there are many tools and equipment used to make sure this project will be done smoothly until it success till the end of the project such as vernier caliper, CNC milling machine, EDM wire cut, drilling machine and etc.

3.3.1 Vernier Caliper

Vernier caliper like Figure 3.2 below is use to measure the dimension of the workpiece before and after cut into the desired dimension. It also uses to measure the thickness and depth of cut for every cutting process finish.

Figure 3.2: Vernier caliper

3.3.2 CNC Milling

The machine that we usually use in this experiment and the main equipment in this project is CNC milling HAAS VF-6 that have in the FKM laboratoty in Universiti Malaysia Pahang (UMP) as shown in Figure 3.3. Table 3.3 show the specification of CNC Milling HAAS VF-6.

Figure 3.3: CNC milling HAAS VF-6

Table 3.3: Specification of CNC Milling HAAS VF-6

TRAVELS	Metric
X Axis	1016 mm
Y Axis	406 mm

Z Axis	406 mm
Spindle Nose to Table (~ min)	102 mm
Spindle Nose to Table (~ max)	508 mm
TABLE	**Metric**
Length	1466.9 mm
Width	267 mm
T-Slot Width	16 mm
T-Slot Center Distance	101.6 mm
Max Weight on Table (evenly distributed)	454 kg
SPINDLE	**Metric**
Max Rating	5.6 kW
Max Speed	4000 rpm
Max Torque	45 Nm @ 1200 rpm
FEEDRATES	**Metric**
Rapids on X	5.1 m/min
Rapids on Y	5.1 m/min
Rapids on Z	5.1 m/min
Max Cutting	5.1 m/min
TOOL CHANGER (OPT)	**Metric**
Capacity	10
Max Tool Diameter (full)	89 mm
Max Tool Weight	5.4 kg
Tool-to-Tool (avg)	5.7 sec
GENERAL	**Metric**
Air Required	113 L/min, 6.9 bar
Power (options may increase requirement)	195-250 VAC/50 A 366-425 VAC/20 A
Machine Weight	1678 kg

Source: Globalspec.com

3.3.3 Cutting Tool

The cutting tool used in this study is a 0◦ lead-positive end milling cutter of 31.75mm diameter. The end mill can be equipped with two square inserts whose all four edges can be used for cutting. The tool inserts were made by Kennametal and had an ISO catalogue number of SPCB120308 (KC735M). In this study, only one inserts per one experiment was mounted on the cutter. The insert had a square shape, back rake angle of 0◦, clearance angle of 11◦, and nose radius of 0.794mm and had no chip breaker. KC735M inserts are coated with a single layer of TiN. The coating is accomplished using PVD techniques to a maximum of 0.004mm thickness. Figure 2.8 shows the TiN insert coated carbide cutting tools used in this study.

Figure 3.4: TiN insert coated carbide attached to the tool holder 2-flute

Each experiment was repeated three times using a new cutting edge every time to obtain very accurate readings of the cutting power. A cutting pass was conducted in such a way that a shoulder, of depth ranging from 1 to 2 mm, and width of 2 to 5 mm, was produced.

3.3.4 Dynometer

The function of dynamometer in this study is to detect the response at x, y and z-axis. The data about cutting power component was acquired with the aid of a piezoelectric cutting power dynamometer. Figure 3.5 below shows the dynamometer been used in study.

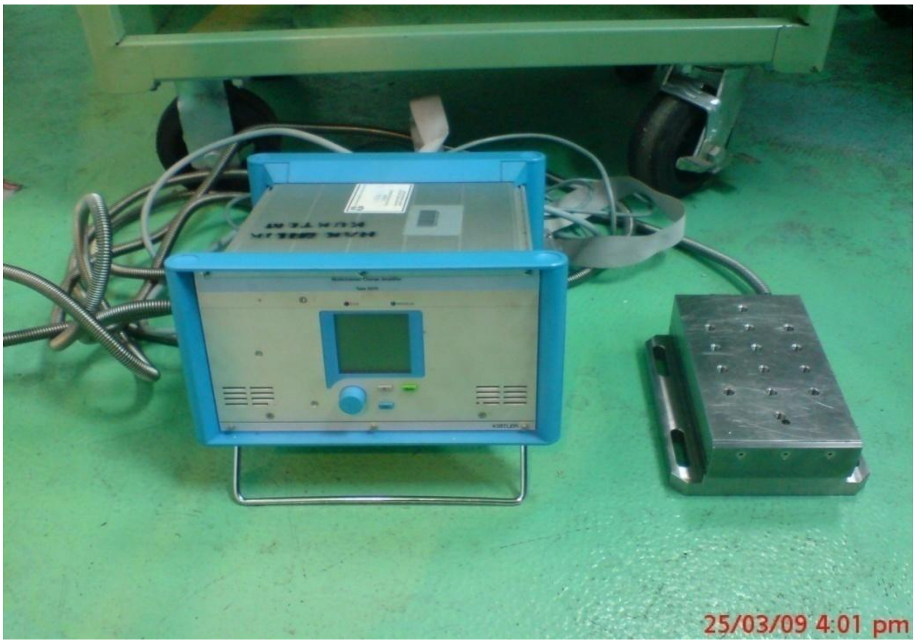

Figure 3.5: Dynometer been used to measure the cutting force

3.4 DESIGN OF EXPERIMENT

The response surface method (RSM) is practical, economical and relatively easy for use. The experimental data was utilized to build mathematical model for first- and second-order model, by regression method using MINITAB software. To generate the table, firstly we must select Response Surface as our Design of Experiment, DOE. Then, create Response Surface Design as shown Figure 3.6 below.

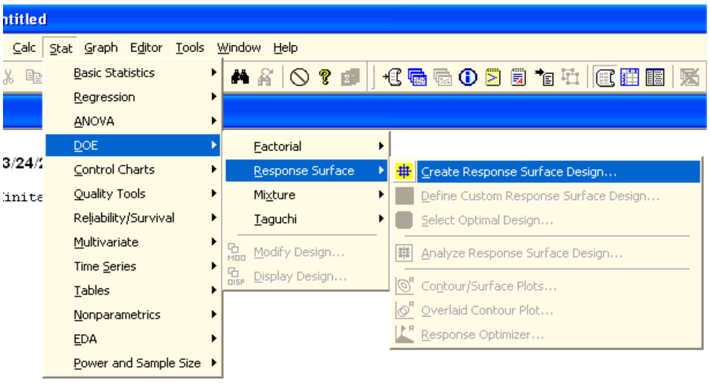

Figure 3.6: Steps to create Response Surface Design

Choose type of design is Box Behnken within 3 to 7 factors. Type the number of factor is 4 since our factors is cutting speed, federate, axial and radial depth of cut. Next, click Display Available Design to predict the number of runs. Since in this study has 4 factors and the design is unblocked Box-Behnken, so we estimate that in this study consist of 27 number of runs. Figure 3.7 below shows the steps.

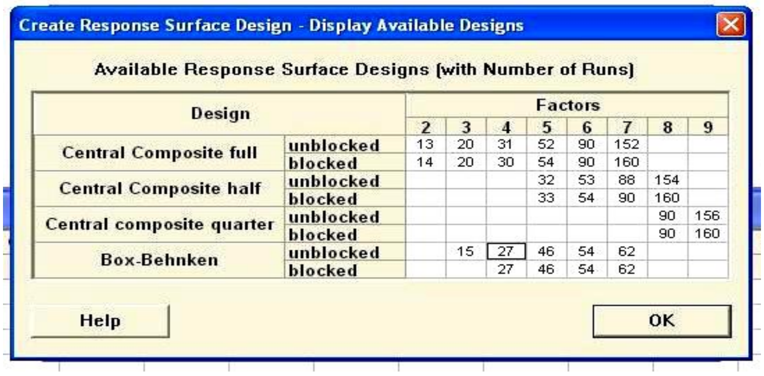

Figure 3.7: 27 number of experiment runs

Number of center points should be default: 3, the number of blocks is 1 and the number of replicates also 1. Next is filling the type of factors and low and high of parameters. For high parameter of cutting speed is 180m/min whereas the low is 100m/min. For high parameter of feedrate is 0.2mm/tooth whereas the low is 0.1mm/tooth. For high parameter of axial depth of cut is 2mm whereas the low is 1mm. For high parameter of radial depth of cut is 5mm whereas the low is 2mm. Figure 3.8 below shows the steps.

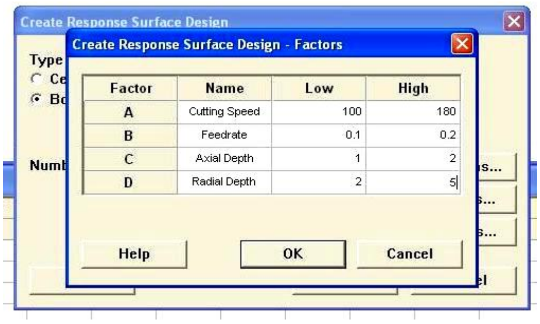

Figure 3.8: Parameters and its low and high range

Mark the randomize runs and store design in worksheet and final step mark printed result as summary table. Figure 3.9 below shows the table generated for 27 experiments.

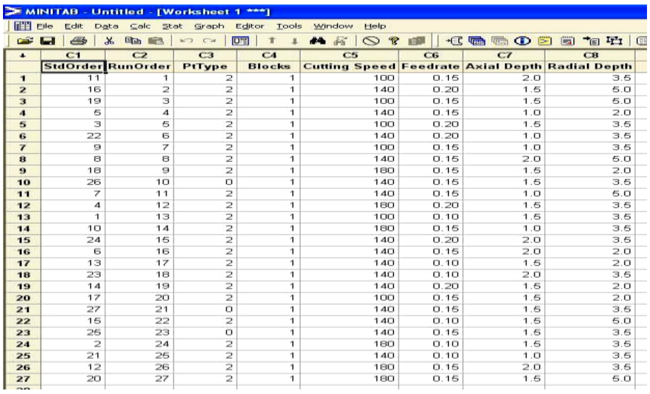

	C1 StdOrder	C2 RunOrder	C3 PtType	C4 Blocks	C5 Cutting Speed	C6 Feedrate	C7 Axial Depth	C8 Radial Depth
1	11	1	2	1	100	0.15	2.0	3.5
2	16	2	2	1	140	0.20	1.5	5.0
3	19	3	2	1	100	0.15	1.5	5.0
4	5	4	2	1	140	0.15	1.0	2.0
5	3	5	2	1	100	0.20	1.5	3.5
6	22	6	2	1	140	0.20	1.0	3.5
7	9	7	2	1	100	0.15	1.0	3.5
8	8	8	2	1	140	0.15	2.0	5.0
9	18	9	2	1	180	0.15	1.5	2.0
10	26	10	0	1	140	0.15	1.5	3.5
11	7	11	2	1	140	0.15	1.0	5.0
12	4	12	2	1	180	0.20	1.5	3.5
13	1	13	2	1	100	0.10	1.5	3.5
14	10	14	2	1	180	0.15	1.0	3.5
15	24	15	2	1	140	0.20	2.0	3.5
16	6	16	2	1	140	0.15	2.0	2.0
17	13	17	2	1	140	0.10	1.5	2.0
18	23	18	2	1	140	0.10	2.0	3.5
19	14	19	2	1	140	0.20	1.5	2.0
20	17	20	2	1	100	0.15	1.5	2.0
21	27	21	0	1	140	0.15	1.5	3.5
22	15	22	2	1	140	0.10	1.5	5.0
23	25	23	0	1	140	0.15	1.5	3.5
24	2	24	2	1	180	0.10	1.5	3.5
25	21	25	2	1	140	0.10	1.0	3.5
26	12	26	2	1	180	0.15	2.0	3.5
27	20	27	2	1	180	0.15	1.5	5.0

Figure 3.9: The table was generated for 27 experiments

The Box–Behnken design is normally used for non-sequential experimentation, when a test is conducted only once. It allows an efficient evaluation of the parameters in the first and second order models. Using Minitab the cutting conditions of 27 experiments are generated and the experiments are conducted randomly to minimize the chance errors. In order to calculate the experimental error, the 27 experiments consider five times repeating of the central point of the cutting conditions. After a series of preliminary trial tests had been conducted and based on the recommendations given by the tool and workpiece manufacturers, the cutting conditions of the main experiments were established as shown in Table 3.4 below.

Table 3.4: Conditions of cutting experiments according to Box–Behnken design

Experiment number	**Cutting speed, *cs* (m/min)**	**Feedrate, *fr* (mm/tooth)**	**Axial depth, *ad* (mm)**	**Radial depth, *rd* (mm)**
1	140	0.15	1	2
2	140	0.2	1	3.5
3	100	0.15	1	3.5
4	180	0.15	1	3.5
5	140	0.1	1	3.5

6	140	0.15	1	5
7	100	0.15	1.5	2
8	140	0.1	1.5	2
9	100	0.2	1.5	3.5
10	140	0.15	1.5	3.5
11	180	0.2	1.5	3.5
12	180	0.15	1.5	2
13	140	0.2	1.5	2
14	140	0.2	1.5	5
15	140	0.15	1.5	3.5
16	180	0.1	1.5	3.5
17	100	0.1	1.5	3.5
18	100	0.15	1.5	5
19	140	0.1	1.5	5
20	180	0.15	1.5	5
21	140	0.15	1.5	3.5
22	140	0.15	2	5
23	140	0.2	2	3.5
24	140	0.1	2	3.5
25	140	0.15	2	2
26	100	0.15	2	3.5
27	180	0.15	2	3.5

In order to reduce the total number of cutting tests and allow simultaneous variation of the four independent factors, a well-designed experimental procedure has to be followed. In machining research, the Box–Behnken design has found a broad application compared to other experiment designs used for RSM. The Box Behnken design is based on the combination of the factorial with incomplete block designs. It does not require a large number of tests as it considers only three levels (−1, 0, 1) of each independent parameter (G.E.P. Box and D.W. Behnken. 1960). Table 3.5 below shows the levels of the four inputs independent.

Table 3.5: Levels of independent variables

Factors	**Coding of levels**		
	-1	**0**	**1**
Cutting speed, *cs* (m/min)	100	140	180
Feedrate, *fr* (mm/tooth)	0.1	0.15	0.2
Axial depth of cut, *ad* (mm)	1	1.5	2
Radial depth of cut, *rd* (mm)	2	3.5	5

Force been measured from dynamometer during machining. Table 3.6 shows the experiment result for cutting force.

Table 3.6: Experiment result for cutting force

Experiment number	**Cutting speed, *cs* (m/min)**	**Feedrate, *fr* (mm/tooth)**	**Axial depth, *ad* (mm)**	**Radial depth, *rd* (mm)**	**Cutting force, F_C (N)**
1	140	0.15	1	2	146.67
2	140	0.2	1	3.5	190.00
3	100	0.15	1	3.5	190.00
4	180	0.15	1	3.5	170.00
5	140	0.1	1	3.5	110.00
6	140	0.15	1	5	225.00
7	100	0.15	1.5	2	240.00
8	140	0.1	1.5	2	100.00
9	100	0.2	1.5	3.5	340.00
10	140	0.15	1.5	3.5	220.00
11	180	0.2	1.5	3.5	293.33
12	180	0.15	1.5	2	145.00
13	140	0.2	1.5	2	200.00
14	140	0.2	1.5	5	325.00
15	140	0.15	1.5	3.5	200.00
16	180	0.1	1.5	3.5	130.00
17	100	0.1	1.5	3.5	190.00
18	100	0.15	1.5	5	340.00
19	140	0.1	1.5	5	210.00
20	180	0.15	1.5	5	240.00
21	140	0.15	1.5	3.5	200.00
22	140	0.15	2	5	350.00
23	140	0.2	2	3.5	350.00
24	140	0.1	2	3.5	200.00
25	140	0.15	2	2	190.00
26	100	0.15	2	3.5	340.00
27	180	0.15	2	3.5	313.33

CHAPTER 4

RESULT AND DISCUSSION

4.1 INTRODUCTION

With reference to the response surface method, where the response variable is the cutting force in this study, the relationship between the investigated four cutting conditions and the response can be represented by the following linear equation such Equation 4.1 below.

$$\ln F = A \ln cs + B \ln fr + C \ln ad + D \ln rd + E \tag{4.1}$$

where F is the cutting force (response), A, B, C, D and E are constants, while cs is cutting speed (m/min), fr is feedrate (mm/rev), ad is axial depth of cut (mm) and rd is the radial depth of cut (mm). Equation 4.1 can be written as Equation 4.2 below:

$$y = \beta_0 x_0 + \beta_1 x_1 + \beta_2 x_2 + \beta_3 x_3 + \beta_4 x_4 + \varepsilon \text{ or}$$
$$\hat{y} = y - \varepsilon = \beta_0 x_0 + \beta_1 x_1 + \beta_2 x_2 + \beta_3 x_3 + \beta_4 x_4 \tag{4.2}$$

where y is the cutting force experimental value and $\hat{y}$ is the predicted value, while x_0, x_1, x_2, x_3, x_4 and ε are dummy variable ($x_0 = 1$), cutting speed, feed rate, axial depth of cut, radial depth of cut, and experimental error, respectively. β_0, β_1, β_2, β_3 and β_4 are the model parameters. In most cases, the response surface variables demonstrate some curvature in most ranges of the cutting parameters. Therefore, it would be useful to consider also the second order model in this study. The second order model helps understand the second order effect of each factor separately and the two-way interaction amongst these factors combined. This model can be represented by the following Equation 4.3.

$$\hat{y}'' = \beta_0 x_0 + \beta_1 x_1 + \beta_2 x_2 + \beta_3 x_3 + \beta_4 x_4 + \beta_{11} x^2_1 + \beta_{22} x^2_2 + \beta_{33} x^2_3 + \beta_{44} x^2_4 + \beta_{12} x_1 x_2 + \beta_{13} x_1 x_3 + \beta_{14} x_1 x_4 + \beta_{23} x_2 x_3 + \beta_{24} x_2 x_4 + \beta_{34} x_3 x_4 \quad (4.3)$$

4.2 RESULT AND DISCUSSION

4.2.1 Development of First Order Cutting Force Model

After conducting the first passes which is one pass is equal to 85mm length of the 27 cutting experiments, the cutting force readings are used to find the parameters appearing in the postulated first order model Equation 4.2. Figure 4.1 below shows the normal probability plot of the residual generated from MINITAB based on first order linear equation.

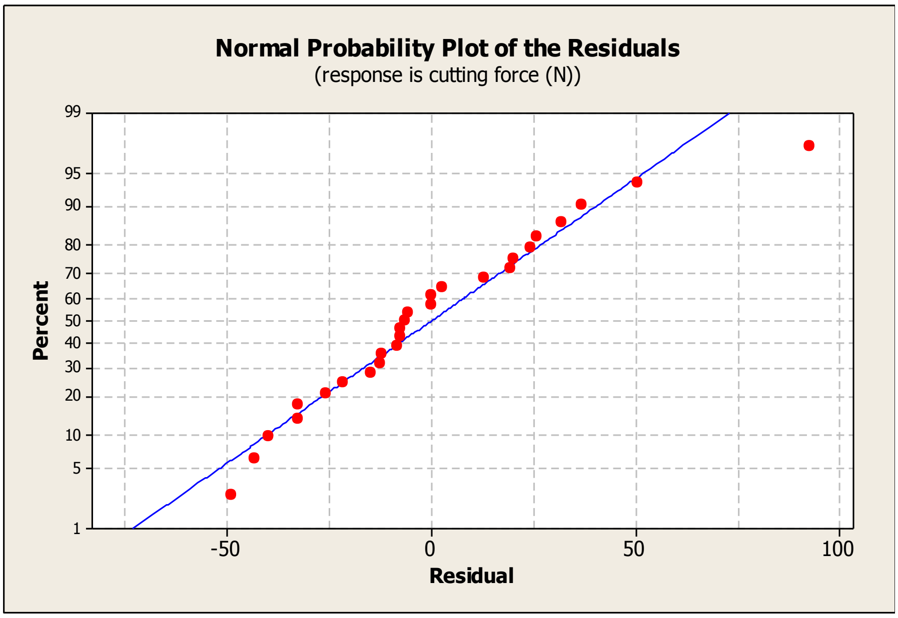

Figure 4.1: The normal probability plot of 1st order model

To do the calculation of these parameters, the method of least squares is used with the aid of MINITAB. Table 4.1 below shows estimated regression coefficients for cutting force (N) using data in uncoded units.

Table 4.1: Estimated Regression Coefficients for Cutting Force (N) using data in uncoded units

Term	Coefficient
Constant	-177.512
Cutting Speed (m/min)	-0.725708
Feedrate (mm/rev)	1316.29
Axial Depth (mm)	118.610
Radial Depth (mm)	38.8762

Next, the first order linear equation for predicting the cutting force can be expressed as Equation 4.4 below.

$$\hat{y} = -177.512 - 0.725708x_1 + 1316.29x_2 + 118.610x_3 + 38.8762x_4 \quad (4.4)$$

From this linear equation, one can easily notice that the response $\hat{y}$ (cutting force) is affected significantly by the feed rate followed by the axial depth of cut and then by the radial depth of cut, and lastly, by the cutting speed. Generally, the increase in the feed rate, axial and radial depths of cut will cause the cutting force to become larger. The negative sign of cutting speed shows that the decrease of the value will cause the cutting force to be increase. This is because when the cutting speed is low, the movement of the cutting tool is low according to time travel and it gives so much pressure to the workpiece while passing through an 85mm length. The proposed linear equation is valid only for cutting modified AISI P20 with a 0◦ lead end mill equipped with TiN coated KC735M carbide inserts and within the cutting conditions ranges used in the experimentation. Table 4.2 below shows the cutting force values received by experimentation and the values predicted by the first order model.

Table 4.2: Comparison between experiment reading of cutting force and predicted results generated by first order model

Experiment number	**Cutting speed, *cs* (m/min)**	**Feedrate, *fr* (mm/tooth)**	**Axial depth, *ad* (mm)**	**Radial depth, *rd* (mm)**	**Experimental result, F_y (N)**	**Predicted result, F_y (N)**
1	140	0.15	1	2	146.67	114.694
2	140	0.2	1	3.5	190.00	238.823
3	100	0.15	1	3.5	190.00	202.037
4	180	0.15	1	3.5	170.00	143.980
5	140	0.1	1	3.5	110.00	107.194
6	140	0.15	1	5	225.00	231.323
7	100	0.15	1.5	2	240.00	203.027
8	140	0.1	1.5	2	100.00	108.185
9	100	0.2	1.5	3.5	340.00	327.156
10	140	0.15	1.5	3.5	220.00	232.313
11	180	0.2	1.5	3.5	293.33	269.099
12	180	0.15	1.5	2	145.00	144.971
13	140	0.2	1.5	2	200.00	239.813
14	140	0.2	1.5	5	325.00	232.313
15	140	0.15	1.5	3.5	200.00	232.313
16	180	0.1	1.5	3.5	130.00	137.471
17	100	0.1	1.5	3.5	190.00	195.527
18	100	0.15	1.5	5	340.00	319.656
19	140	0.1	1.5	5	210.00	224.813
20	180	0.15	1.5	5	240.00	261.599
21	140	0.15	1.5	3.5	200.00	232.313
22	140	0.15	2	5	350.00	349.933
23	140	0.2	2	3.5	350.00	357.433
24	140	0.1	2	3.5	200.00	225.804
25	140	0.15	2	2	190.00	233.304
26	100	0.15	2	3.5	340.00	320.647
27	180	0.15	2	3.5	313.33	262.590

It is obvious that the predicted values are very close to the experimental readings. This indicates that the obtained linear model is able to provide, to a great extent, accurate values of cutting force. The adequacy of the first order model was verified using the analysis of variance (ANOVA). ANOVA was performed to determine the significant and non-significant parameters as well as the validity of the full models. The ANOVA was carried out on each model for a confidence level of 95% (N.S.M. El-Tayeb *et al*, 2009). The lack-of-fit *F*-value of 0.22 is not significant with relative to the pure error and this implies that the model could fit and it is sufficient. There is about a chance of 98.6% that the lack-of-fit *F*-value could occur due to noise as shown in Table 4.3 below.

Table 4.3: Analysis of variance ANOVA for first order equation generated from Minitab

Source of variation	**Degree of freedom (d.f.)**	**Sum of squares (SS)**	**Mean squares (MS)**	***F***	***P***
Zero order term	4	129123	32280.8	27.73	0
Residual error	22	25609	1164.1		
Lack-of-fit	19	14841	781.1	0.22	0.986
Pure error	3	10769	3589.6		
Total	26	154733			

The developed linear model equation 4.4 was used to plot contours of the cutting force at different values of the axial and radial depths of cut. Figure 4.2 below shows the cutting force contours at three different combinations of the axial and radial depths (lowest "−1", middle "0", and highest values "+1"). It is clear that the increasing in feed rate and decreasing of cutting speed will cause the cutting force to increase dramatically. From Fig. 2(c) below, the cutting force reaches its highest value when all cutting conditions at their maximum values. In this case the cutting speed is at its smallest value (100 m/min).

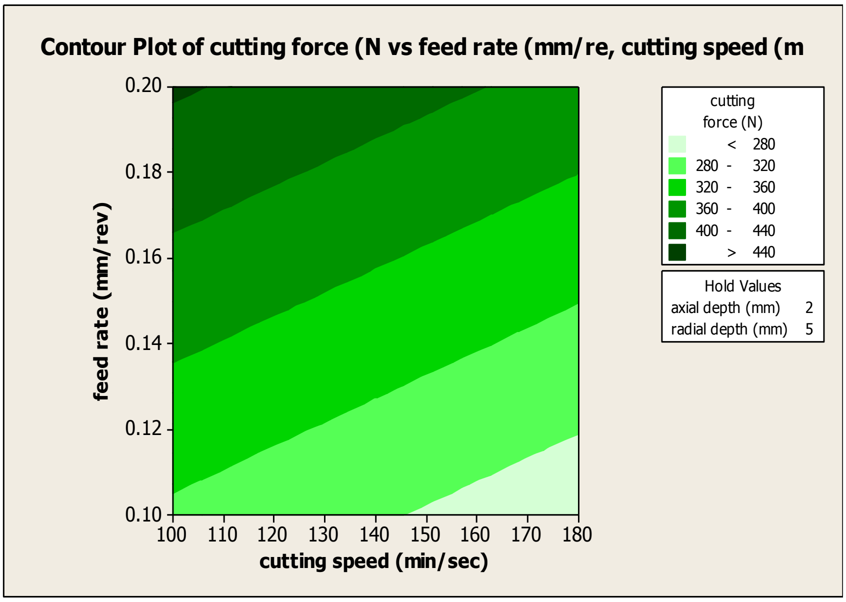

(a) Axial depth=2mm, Radial depth=5mm

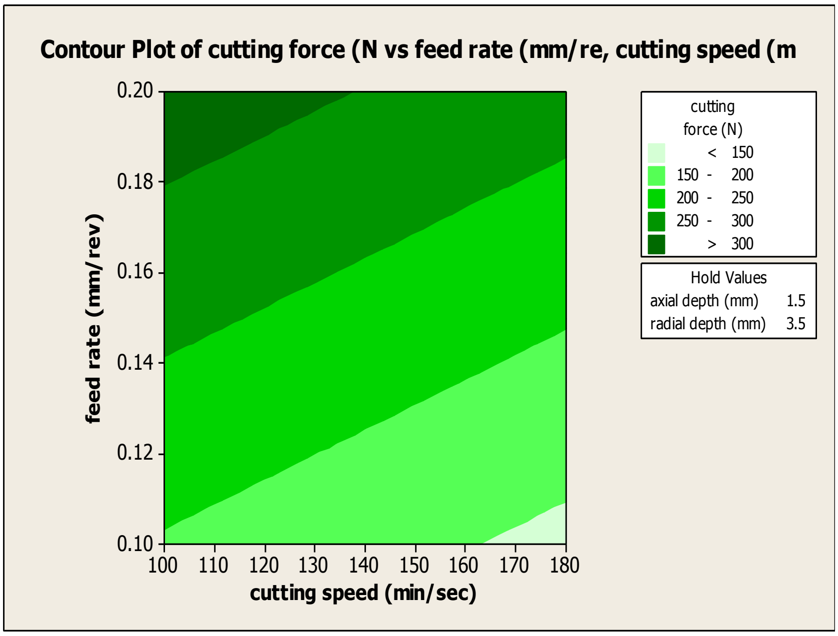

(b) Axial depth=1.5mm, Radial depth=3.5mm

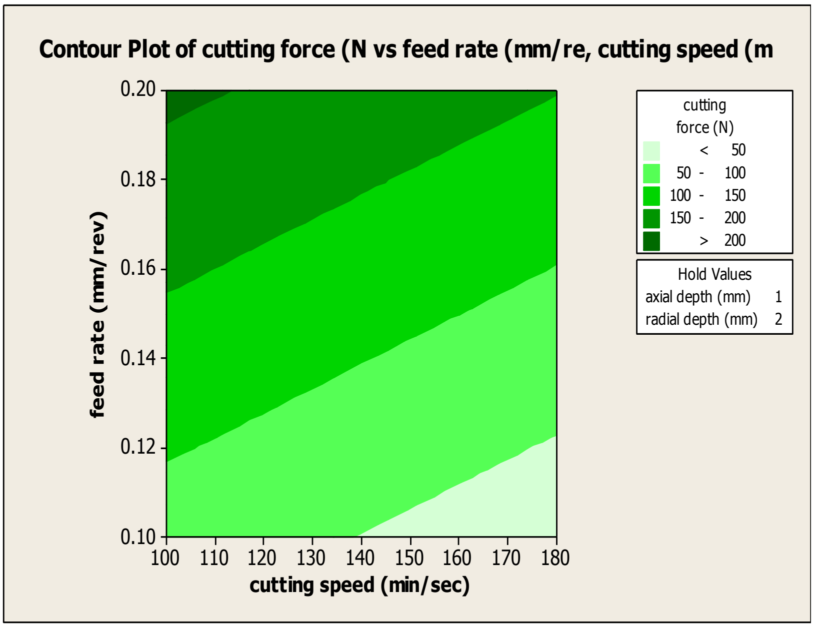

(c) Axial depth=1mm, Radial depth=2mm

Figure 4.2: Cutting force contours in cutting speed–feed plane for different combinations of axial and radial depths of cut plotted from first order model: (a) *ad* =1, *rd* = 2mm (lowest values); (b) *ad* = 1.5, *rd* = 3.5mm (middle values); (c) *ad* =2, *rd* = 5mm (highest values)

To prove that the model is satisfied with the analysis, use the Eq. 4.4 and replace the variables x_1, x_2, x_3 and x_4 with the maximum and minimum value of parameter and the predicted result are in range between 77.9086 N – 386.7196 N. This range is valid according to the predicted result in the Table 4.2 because the predicted values of 27 experiments are in the range of the linear mathematical model developed from RSM.

Table 4.4: Error analysis percentage of first order model

Experiment number	Experimental result, *Fy* (N)	Predicted result, *Fy* (N)	Error Analysis (%)
1	146.67	114.694	21.80
2	190.00	238.823	-25.69
3	190.00	202.037	-6.33
4	170.00	143.980	15.30
5	110.00	107.194	2.55

6	225.00	231.323	-2.81
7	240.00	203.027	15.40
8	100.00	108.185	-8.18
9	340.00	327.156	3.77
10	220.00	232.313	-5.59
11	293.33	269.099	8.26
12	145.00	144.971	0.02
13	200.00	239.813	-19.90
14	325.00	232.313	28.51
15	200.00	232.313	-16.15
16	130.00	137.471	-5.74
17	190.00	195.527	-2.90
18	340.00	319.656	5.98
19	210.00	224.813	-7.053
20	240.00	261.599	-8.99
21	200.00	232.313	-16.15
22	350.00	349.933	0.01
23	350.00	357.433	-2.12
24	200.00	225.804	-12.90
25	190.00	233.304	-22.79
26	340.00	320.647	5.69
27	313.33	262.590	16.19

In numerical simulation or modeling of real systems, error analysis is concerned with the changes in the output of the model as the parameters to the model vary about a mean. The error analysis is use to the two outputs in the Table 4.4 to find the percentage of the error between experimental result and predicted result. The percentage of analysis error is formulated as Equation 4.5 as below:

$$\frac{(\text{Experimental value} - \text{Predicted Value})}{\text{Experimental Value}} \times 100\% \qquad (4.5)$$

The Figure 4.3 shows the graph for the range of percentage error of first order model of cutting force. It is accurately predicted that the error analysis percentage range of linear equation model is between –25.69% and 28.51%.

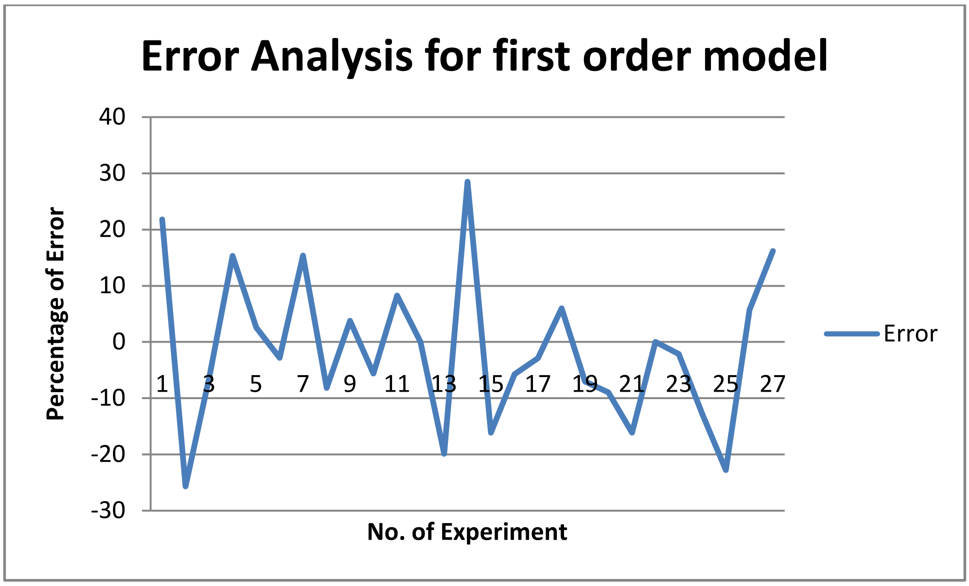

Figure 4.3: The graph of error analysis for first order model

4.3.2 Development of Second Order Cutting Force Model

The second order equation was established to describe the effect of the four cutting conditions investigated in this study on the cutting force. Figure 4.4 below shows the normal probability plot of 2^{nd} order model generated from MINITAB based on second order equation.

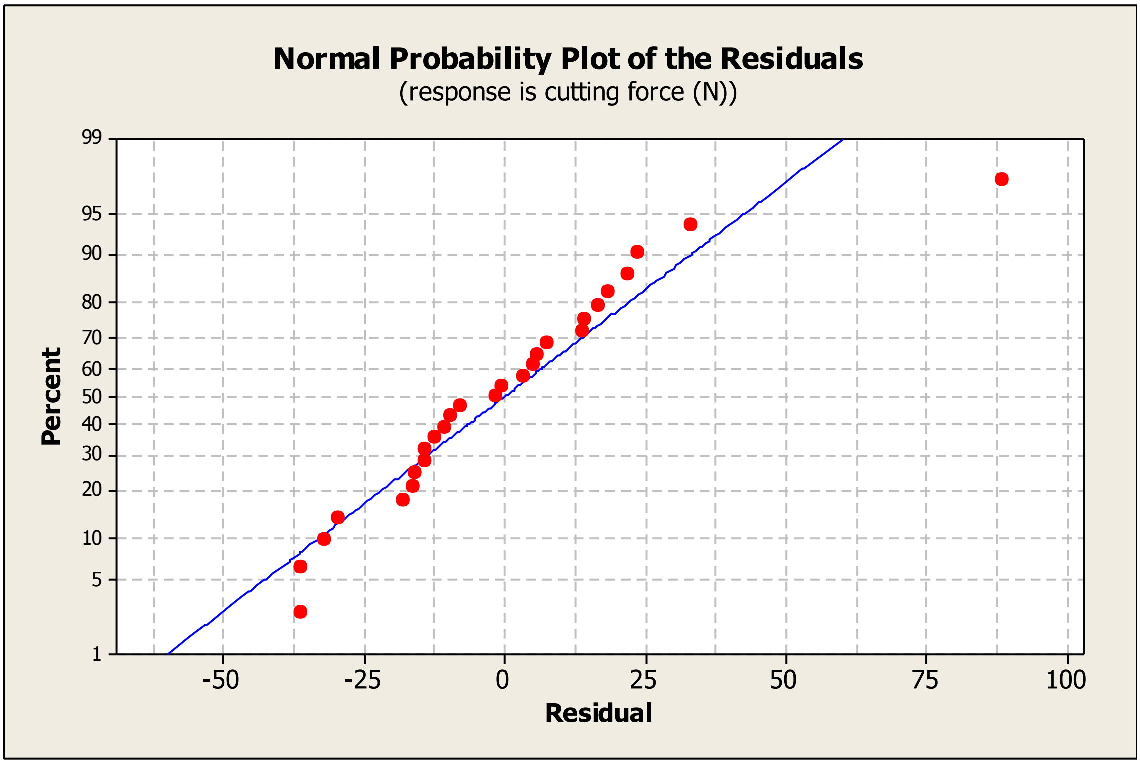

Figure 4.4: The normal probability plot of 2nd order model

Table 4.5 below shows estimated regression coefficients for cutting force (N) using data in uncoded units.

Table 4.5: Estimated Regression Coefficients for force (N) using data in uncoded units

Term	Coefficient
Constant	182.562
Cutting Speed (m/min)	-3.82547
Feedrate (mm/rev)	1773.99
Axial Depth (mm)	-44.0012
Radial Depth (mm)	11.6913
Cutting Speed (m/min)*Cutting Speed (m/min)	0.0108850
Feedrate (mm/rev)*Feedrate (mm/rev)	-7016.80
Axial Depth (mm)*Axial Depth (mm)	-8.66600
Radial Depth (mm)*Radial Depth (mm)	-3.72200

Cutting Speed (m/min)*Feedrate (mm/rev)	1.66625
Cutting Speed (m/min)*Axial Depth (mm)	-0.0833750
Cutting Speed (m/min)*Radial Depth (mm)	-0.0208333
Feedrate (mm/rev)*Axial Depth (mm)	700.000
Feedrate (mm/rev)*Radial Depth (mm)	95.5533
Axial Depth (mm)*Radial Depth (mm)	27.2233

Next, the model is obtained using the Box–Behnken design and the Equation 4.5 can be written as below.

$$\hat{y}'' = 182.562 - 3.82547x1 + 1773.99x2 - 44.0012x3 + 11.6913x4 + 0.0108850x^21 - 7016.80x^22 - 8.66600x^23 - 3.72200x^24 + 1.66625x1x2 - 0.0833750x1x3 - 0.0208333x1x4 + 700.000x2x3 + 95.5533x2x4 + 27.2233x3x4$$
(4.5)

The model shows that the cutting force increases with increasing the feed rate but it decreased if cutting speed is reduced. On the other hand, unlike in the case of the first order model, the axial depth of cut, as a separate factor, has a negative effect. The increase in axial depth of cut will cause a reduction in the cutting force. Anyway, this effect may be not noticed if we take inconsideration its interaction with the feed rate. One can easily see from this equation is that the interaction of the feed rate with axial depth of cut is extremely high. It is noticed that this interaction has the most dominant effect on the cutting force. The cutting force readings obtained experimentally and predicted values by this equation are shown in Table 4.6. It can be concluded from the table that the equation can produce values close to those found experimentally. The analysis of variance shown in Table 4.7 indicates that the model is adequate as the *P*-values of the lack-of-fit are not significant.

Table 4.6: Comparison between experiment reading of cutting force and predicted results generated by second order model

Experiment number	Cutting speed, *cs* (m/min)	Feedrate, *fr* (mm/tooth)	Axial depth, *ad* (mm)	Radial depth, *rd* (mm)	Experimental result, *Fy* (N)	Predicted result, *Fy* (N)
1	140	0.15	1	2	146.67	129.988
2	140	0.2	1	3.5	190.00	204.070
3	100	0.15	1	3.5	190.00	219.555
4	180	0.15	1	3.5	170.00	164.834
5	140	0.1	1	3.5	110.00	110.404
6	140	0.15	1	5	225.00	202.820
7	100	0.15	1.5	2	240.00	216.237
8	140	0.1	1.5	2	100.00	96.334
9	100	0.2	1.5	3.5	340.00	326.153
10	140	0.15	1.5	3.5	220.00	236.250
11	180	0.2	1.5	3.5	293.33	274.761
12	180	0.15	1.5	2	145.00	160.680
13	140	0.2	1.5	2	200.00	210.667
14	140	0.2	1.5	5	325.00	236.250
15	140	0.15	1.5	3.5	200.00	236.250
16	180	0.1	1.5	3.5	130.00	139.430
17	100	0.1	1.5	3.5	190.00	204.152
18	100	0.15	1.5	5	340.00	332.403
19	140	0.1	1.5	5	210.00	195.667
20	180	0.15	1.5	5	240.00	271.846
21	140	0.15	1.5	3.5	200.00	280.109
22	140	0.15	2	5	350.00	362.265
23	140	0.2	2	3.5	350.00	357.680
24	140	0.1	2	3.5	200.00	194.014
25	140	0.15	2	2	190.00	207.764
26	100	0.15	2	3.5	340.00	341.500
27	180	0.15	2	3.5	313.33	280.109

It can be concluded from the table that the equation can produce values close to those found experimentally. The analysis of variance shown in Table 4.7 below indicates that the model is adequate as the *P*-values of the lack-of-fit are not significant.

Table 4.7: Analysis of variance ANOVA for second order equation from Minitab

Source of variation	Degree of freedom (d.f.)	Sum of squares (SS)	Mean squares (MS)	*F*	*P*
Regression	14	137388	9813.4	6.79	0.001
First order term	4	129123	28893.4	19.99	0.000
Second order term	4	5182	1131.2	0.78	0.558
Interaction terms	6	3083	513.8	0.36	0.893
Residual error	12	17345	1445.4		
Lack-of-fit	10	6576	730.7	0.20	0.973
Pure error	2	10769	3589.6		
Total	26	154733			

According to the ANOVA for the first and second order, it shows that the lack-of-fit of first order equation (0.986) is bigger than the second order equation (0.973). It shows that the linear equation of cutting force prediction is more appropriate to use compare with the quadratic equation model. The higher lack-of-fit we get the higher percentage of accuracy the value of predicted value to the reference line in the normal probability graph.

Figure 4.5 below shows the contour plots of the cutting force in the cutting speed and feed plane of the lowest, middle and highest values of the axial and radial depth of cut. As it was concluded before in the linear model, the cutting force increases with the increasing federate, and goes along with the axial and radial depth. However, it is indirectly proportional to the cutting speed.

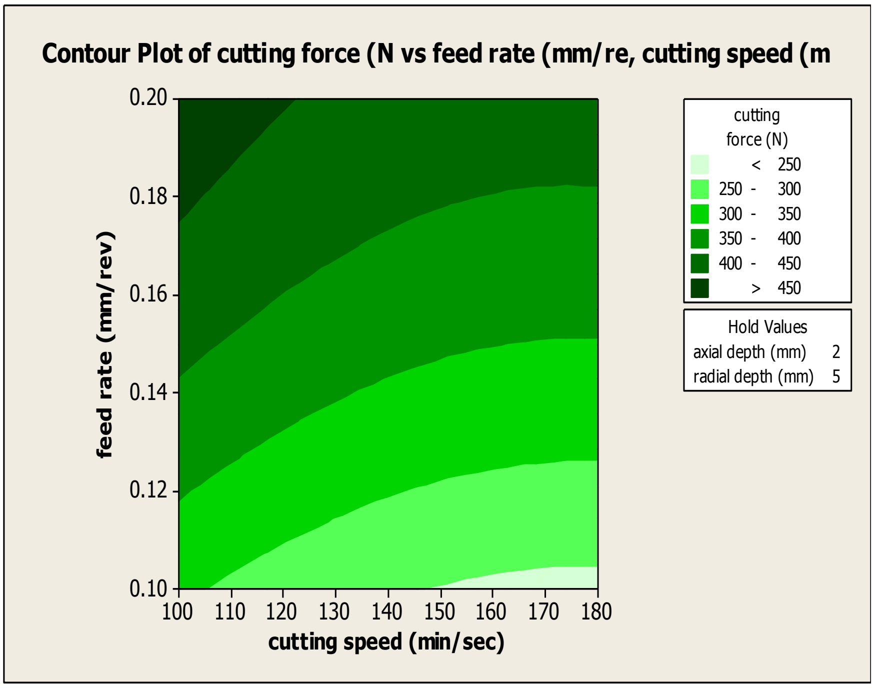

(a) Axial depth=1mm, Radial depth=2mm

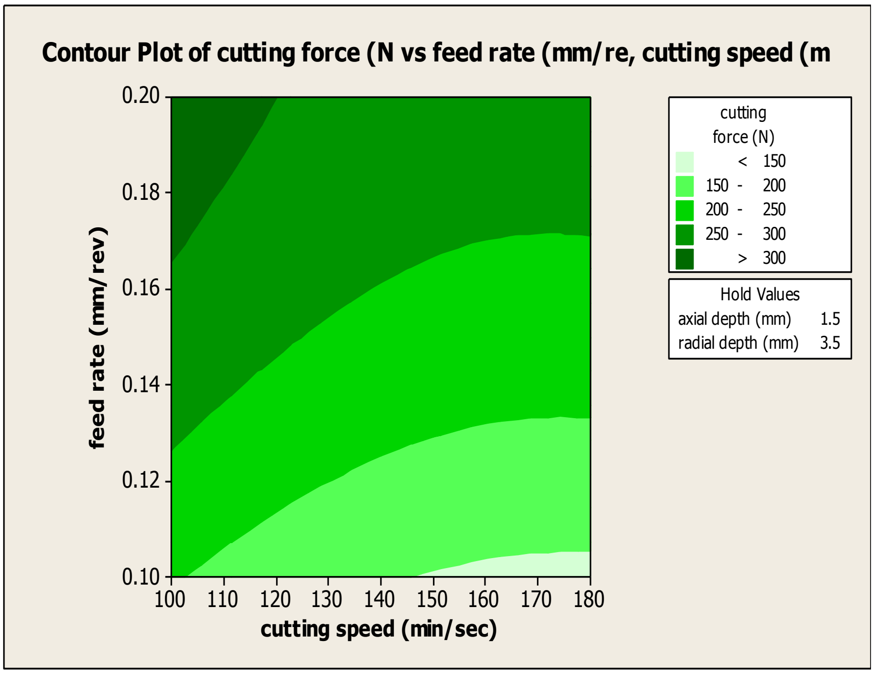

(b) Axial depth=1.5mm, Radial depth=3.5mm

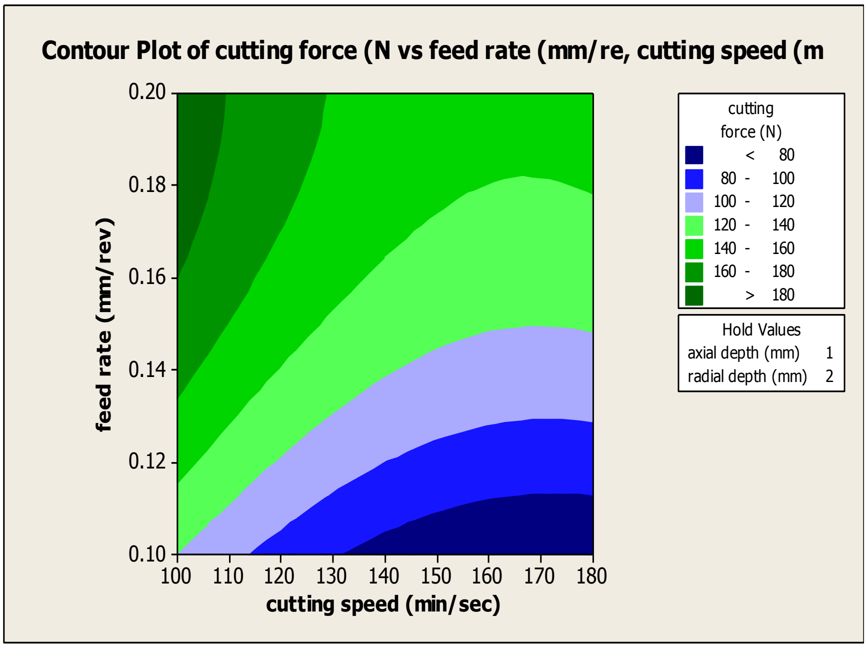

(c) Axial depth = 2mm, Radial depth = 5mm

Figure 4.5: Cutting force contours in cutting speed–feed plane for different combinations of axial and radial depths of cut plotted from second order model: (a) *ad* =1, *rd* = 2mm (lowest values); (b) *ad* = 1.5, *rd* = 3.5mm (middle values); (c) *ad* =2, *rd* = 5mm (highest values)

To prove that the model is satisfied with the analysis, use the Eq. 4.5 and replace the variables x_1, x_2, x_3 and etc with the maximum and minimum value of parameter and the predicted result are in range between.7497 N – 242.5238 N. This range is valid according to the predicted result in the Table 4.6 because the predicted values of 27 experiments are in the range of the linear mathematical model developed from RSM.

Table 4.8: Error analysis percentage of second order model

Experiment number	Experimental result, *Fy* (N)	Predicted result, *Fy* (N)	Error Analysis (%)
1	146.67	129.988	11.37
2	190.00	204.070	-7.41
3	190.00	219.555	-15.55

4	170.00	164.834	3.04
5	110.00	110.404	-0.37
6	225.00	202.820	9.85
7	240.00	216.237	9.90
8	100.00	96.334	3.66
9	340.00	326.153	4.07
10	220.00	236.250	-7.38
11	293.33	274.761	6.33
12	145.00	160.680	-10.81
13	200.00	210.667	-5.33
14	325.00	236.250	27.31
15	200.00	236.250	-18.13
16	130.00	139.430	-7.25
17	190.00	204.152	-7.44
18	340.00	332.403	2.23
19	210.00	195.667	6.82
20	240.00	271.846	-13.26
21	200.00	280.109	-40.05
22	350.00	362.265	-3.50
23	350.00	357.680	-2.19
24	200.00	194.014	2.99
25	190.00	207.764	-9.34
26	340.00	341.500	-0.44
27	313.33	280.109	10.60

The error analysis is use to the two outputs in the Table 4.8 to find the percentage of the error between experimental result and predicted result. The percentage of analysis error is formulated as Eq. 4.5. The graph of Figure 4.6 shows the range of percentage error of first order model of cutting force. It is accurately predicted that the error analysis percentage range of quadratic equation model is between –40.05% and 27.31%. It is clear that the range of percentage error of second order is bigger than first order model analysis. It shows that the second order model is less suitable model to consider in calculation because the error that will occur is more than first order.

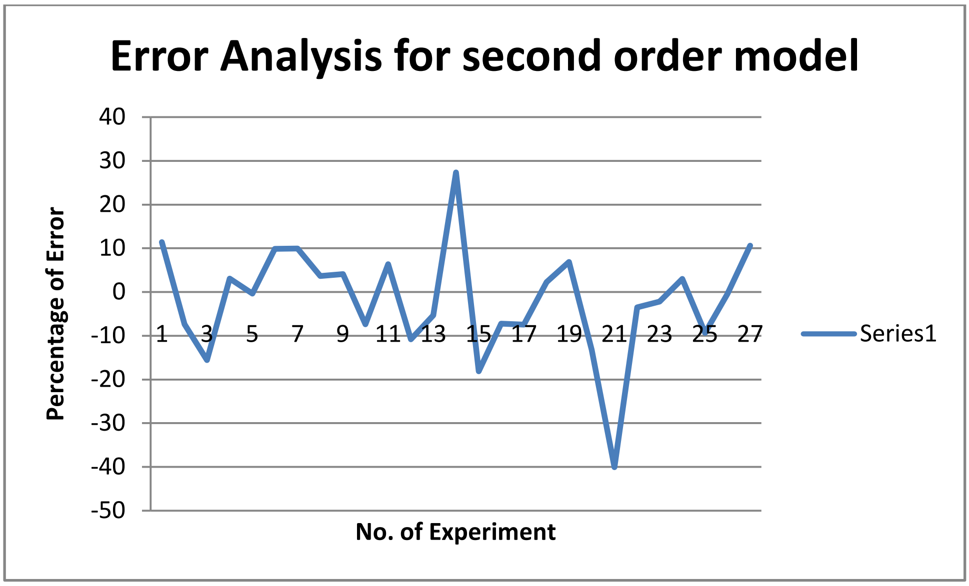

Figure 4.6: The graph of error analysis for second order model

CHAPTER 5

CONCLUSION

5.1 CONCLUSION

In conclusion, by using RSM (response surface method) the objectives of this project is successfully done. The first and second order models of predicted cutting force are generated in Minitab Software are able to provide accurately predicted values of the cutting power close to those values found in the experiments. With a confidence interval of 95%, the mathematical models are found competence to the experiment value. Thus the prediction of cutting force, Fy produced in end milling of modified AISI P20 with TiN coated inserts mounted on 0◦ lead cutters is successfully obtained by RSM.

According to the ANOVA for the first and second order, it shows that the lack-of-fit of first order equation (0.986) is bigger than the second order equation (0.973). It shows that the linear equation of cutting force prediction is more appropriate to use compare with the quadratic equation model. The higher lack-of-fit we get the higher percentage of accuracy the value of predicted value to the reference line in the normal probability graph. This clarification also proven by the error analysis applied to these two equation models. Error analysis percentage range of linear equation model is between –25.69% and 28.51% while the error analysis percentages range of quadratic equation model is between –40.05% and 27.31%. It shows that the error range of linear equation model is smaller than the quadratic equation model.

The two equations, the first and second order model indicate that the feed rate was the most dominant cutting condition on the cutting force, followed by the axial depth, radial depth of cut and then by the cutting speed. The cutting force increases with increasing the feed rate, depths of cut but decreases with increasing cutting speed. In addition, the second order model proves the existence of a very strong interaction of the feed rate with axial depth of cut. It has been experiential that the improvement in the cutting force through the optimization of input parameters, such as cutting speed, federate, axial and radial depth of cut, may result in a significant economical performance of machining operations.

With a view to achieving the above mentioned aim, statistically designed experiments based on the RSM technique were used to reduce the cost and time involved as well as to obtain the requires information about direct and interaction effects of process parameters on the response parameters. The responses can be effectively controlled by substituting appropriate values of the process variables in to the mathematical model developed. It will help a researcher or individual in industry to manually conduct an experiment by referring the analysis made by this project.

5.2 RECOMMENDATIONS

Use much other method such as Taguchi, Neural Network, Artificial Intelligence, and some others method and do the comparison between each one for further study. Comparison which design of experiment gives more accurate mathematical model between neural network (NN), Taguchi method and response surface method (RSM) in term of cutting force result. It may also include comparisons of error in prediction of cutting force by neural network (NN), Taguchi method and response surface method (RSM) and which one has great potential to be employed in predicting optimum cutting parameter without needing extensive iterative cutting trials. Another study that can be further performed on milling process could possibly be a work that studies the affects of different types of cutting tool compare to the current use 0◦ lead-positive end milling cutter of 31.75mm diameter on the same types of material and the parameters to study is more than 4 variables.

REFERENCES

This thesis is prepared based on the following references;

Alauddin, M., El Baradie, M. A. and Hashmi, M. S. J., “Optimization of surface finish in end milling Inconel 718”, *Journal of Materials Processing Technology,* v 56, n 1-4, 1996, p 54-65

Amago, T., “Sizing optimization using response surface method in First Order analysis”. *R & D Review of Toyota CRDL,* v 37 n 1.

B. Ganesh babu, V. Selladurai and R. Shanmugam. 2008. Analytical Modeling Of Cutting Forces Of End Milling Operation On Aluminum Silicon Carbide Particulate Metal Matrix Composite Material Using Response Surface Methodology, *ARPN Journal of Engineering and Applied Sciences* VOL. 3, NO. 2

Brosheer, B. C. 1948. “How Smooth is Smooth? Part-I, Specification and Evaluation of Machined Finishes”, *American Machinist*, McGrow-Hill Publishing Company, pp. 97-112.

Byrne G, Dornfeld D, Inasaki I, Ketteler G And Teti R, (1995) Tool Conditionmonitoring - The Status Of Research And Industrial Application, *CIRP Annals*, Vol. 44, Pp. 541-567.

D. Bajic, B. Lela, D. @Ivkovic (2008), Modeling Of Machined Surface Roughness And Optimization Of Cutting Parameters In Face Milling, *Metalurgija* 47 (2008) 4, 331-334

D.C. Montgomery. 2001. Design and Analysis of Experiments (5th ed.), John Wiley & Sons Inc, New York

D.I. Lalwani, N.K. Metha and P.K. Jain. 2008. Experimental investigations of cutting parameters influence on cutting forces and surface roughness in finish hard turning of MDN250 steel, *Journal of Materials Processing Technology,* Volume 206, Issues 1-3, 12 September 2008, Pages 167-179

Dr. Mike S. Lou, Dr. Joseph C. Chen & Dr. Caleb M. Li. 1998. Surface Roughness Prediction Technique for CNC End-Milling, *Journal of Industrial Engineering, Volume* 15, Number 1

G. Steenackers, F. Presezniak and P. Guillaume. 2009. Development of an adaptive response surface method for optimization of computation-intensive models, *Computers & Industrial Engineering* Volume 57, Issue 3, October 2009, Pages 847-855

H. O¨ ktema,∗, T. Erzurumlu b, H. Kurtaran. 2005. Application of response surface Materials methodology in the optimization of cutting conditions for surface roughness, *Journal of Processing Technology 170* (2005) 11–16

Huynh, V. M. and Fan, Y. 1992. "Surface-Texture Measurement and Characterization with Applications to Machine-Tool Monitoring", *The International Journal of Advanced Manufacturing Technology*, 7, pp.2-10.

http://www.sme.org/cgi-bin/get-file.pl?/gmn/DV/pdf/DV03PUB12.pdf. Retrieved on March 28, 2009.

http://www.diehlsteel.com/t_effects.aspx#c. Retrieved on Nov 10, 2009

http://www.sherline.com/8540pg.htm. Retrieved on Nov 16, 2009

http://www.substech.com/dokuwiki/doku.php?id=die_steel_p20. Retrieved on Nov 10, 2009

I. Korkut, M.A. Donertas, U. Seker. 1999. Three-dimensional dynamometer design and production, Zk¨u, Karab¨uk Technical Education Faculty, *J. Technol*. 2 (1–2) 115–129.

K. Kadirgama, K. A. Abou-El-Hossein, B. Mohammad, M. M. Noor and S. M. Sapuan. 2008. Prediction of tool life by statistic method in end-milling Operation, Scientific Research and Essay Vol. 3 (5), pp. 180-186

K.A. Abou-El-Hossein, K. Kadirgama, M.Hamdi, K.Y. Benyounis. 2007. Prediction of cutting force in end-milling operation of modified AISI P20 tool steel, Journal of Materials Processing Technology 182 (2007) 241–247

Kosmol J. 1995. Tool and Process Monitoring - State of Art and Future Prospects, *Scientific Papers of the Inst. of Mech. Eng. and Automation of the Technical Univ. of Wroclaw*, Vol. 61, pp. 90-112.

Kurt A. Rosentrater, Andrew Otieno, Pratyusha Melampati, Determination of Machining Parameters of Corn Byproduct Filled Plastics, *Proceedings of The 2008 IAJC-IJME International Conference*

Lucas, J.M. 1994. Using response surface methodology to achieve a robust process. *Journal of Quality Technology*, 26(4), 248–260

M.A. El Baradie. 1996. Cutting fluids: Part I. Characterisation, *Journal of Materials Processing Technology* 56 (1–4)

M.C. Shaw, Metal Cutting Principles, Oxford University Press, Oxford, 1986.

Mustafa Gunay, ˙Ihsan Korkut, Ersan Aslan, Ulvi S¸eker, Experimental investigation of the effect of cutting tool rake angle on main cutting force, *Journal of Materials Processing Technology* 166 (2005) 44–49

Montgomery, D.C. and Peck, E.A. 1992. *Introduction to Linear Regression Analysis*, Wiley, New York.

Myers, R.H., Montgomery, D.C. 1995. Response Surface Methodology: Process and Product Optimization Using Designed Experiments. New York, Wiley

N.S.M. El-Tayeb, T.C. Yap, V.C. Venkatesh and P.V. Brevern. 2009. Modeling of cryogenic frictional behaviour of titanium alloys using Response Surface Methodology approach, *Materials & Design*, Volume 30, Issue 10, December 2009, Pages 4023-4034

NAVY-repairmans-manual-Chapter11, Computer Numerical Control Machines

Olivo, C. T. 1987. Machine Tool Technology and Manufacturing Processes, C. Thomas Olivo Association, Albany, NY.

P. J. Ross. 1996. "Taguchi Techniques for Quality Engineering: Loss Function, Orthogonal Experiments, Parameter and Tolerance Design", 2nd Edn., McGraw-Hill, New York

P.S. Sreejith, Machining of 6061 aluminium alloy with MQL, dry and flooded lubricant conditions, *Materials Letters* 62 (2008) 276–278

P. Sahoo, T.K. Barman and B.C. Routara. 2008. Fractal dimension modelling of surface profile and optimisation in CNC end milling using Response Surface Method *Int. J. Manufacturing Research, Vol. 3, No. 3*

P. Thangavel and V. Selladurai. 2008. An experimental investigation on the effect of turning parameters on surface roughness, *Int. J. Manufacturing Research, Vol. 3, No. 3*

Scott A. Daggett," How to Choose the Right Tool Coating for Your Machining Application", *Journal of molding making technology*, 2009.

T. W. Simpson1, J. D. Peplinski2, P. N. Koch3 and J. K. Allen (2001), Metamodels for Computer-based Engineering Design: Survey and recommendations, *Engineering with Computers* (2001) 17: 129–150

Tugrul Özel, Marco Lucchi, Ciro A. Rodríguez And Taylan Altan. 1998. Prediction Of Chip Formation And Cutting Forces In Flat End Milling:Comparison Of Process Simulations With Experiments, *Engineering Research Center For Net Shape Manufacturing (Erc/Nsm),* Volume xxvi

Raviraj Shetty, R. Pai, V. Kamath and S. S. Rao. 2008. Study On Surface Roughness Minimization In Turning Of Dracs Using Surface Roughness Methodology And Taguchi

Under Pressured Steam Jet Approach, *ARPN Journal of Engineering and Applied Sciences*, Vol. 3, No. 1

Williams, J. A. and Tabor, D. 'The role of lubricants in machining' *Wear*, 43, pp275-292 (1977).

Won-Soo Yun, Dong-Woo Cho. 2001. Accurate 3-D cutting force prediction using cutting condition independent coefficients in end milling, *International Journal of Machine Tools & Manufacture* 41 (2001), 463–478

Yakup Yildiz_, Muammer Nalbant. 2008. A review of cryogenic cooling in machining processes, *international journal of machine tools &manufacture*, 48 (2008) 947–964

Yusuf Sahin, A. Riza Motorcu. 2004. Surface roughness model for machining mild steel with coated carbide tool, *Materials and Design* 26 (2005) 321–326

APPENDIX A

Table A: Experiment data collection table

Experiment number	Cutting speed (m/min)	Feedrate (mm/tooth)	Axial depth (mm)	Radial depth (mm)	Power calculated (W)
1	140	0.15	1	2	146.67
2	140	0.2	1	3.5	190.00
3	100	0.15	1	3.5	190.00
4	180	0.15	1	3.5	170.00
5	140	0.1	1	3.5	110.00
6	140	0.15	1	5	225.00
7	100	0.15	1.5	2	240.00
8	140	0.1	1.5	2	100.00
9	100	0.2	1.5	3.5	340.00
10	140	0.15	1.5	3.5	220.00
11	180	0.2	1.5	3.5	293.33
12	180	0.15	1.5	2	145.00
13	140	0.2	1.5	2	200.00
14	140	0.2	1.5	5	325.00
15	140	0.15	1.5	3.5	200.00
16	180	0.1	1.5	3.5	130.00
17	100	0.1	1.5	3.5	190.00
18	100	0.15	1.5	5	340.00
19	140	0.1	1.5	5	210.00
20	180	0.15	1.5	5	240.00
21	140	0.15	1.5	3.5	200.00
22	140	0.15	2	5	350.00
23	140	0.2	2	3.5	350.00
24	140	0.1	2	3.5	200.00
25	140	0.15	2	2	190.00
26	100	0.15	2	3.5	340.00
27	180	0.15	2	3.5	313.33

APPENDIX B

ANOVA result from Minitab for Linear Model.

```
The analysis was done using coded units.

Estimated Regression Coefficients for cutting force (N)

Term                        Coef  SE Coef       T      P
Constant                  232.31    6.591  35.249  0.000
cutting speed (min/sec)  -29.03     9.849  -2.947  0.007
feed rate (mm/rev)        65.81    10.351   6.358  0.000
axial depth (mm)          59.31     9.849   6.021  0.000
radial depth (mm)         58.31    10.351   5.634  0.000

S = 34.12   R-Sq = 83.4%   R-Sq(adj) = 80.4%


Analysis of Variance for cutting force (N)

Source          DF  Seq SS  Adj SS   Adj MS      F      P
Regression       4  129123  129123  32280.8  27.73  0.000
  Linear         4  129123  129123  32280.8  27.73  0.000
Residual Error  22   25609   25609   1164.1
  Lack-of-Fit   19   14841   14841    781.1   0.22  0.986
  Pure Error     3   10769   10769   3589.6
Total           26  154733


Unusual Observations for cutting force (N)

               cutting
                 force
Obs  StdOrder      (N)      Fit  SE Fit  Residual  St Resid
 14        14  325.000  232.313   6.591    92.687      2.77 R

R denotes an observation with a large standardized residual.


Estimated Regression Coefficients for cutting force (N) using data in uncoded
     units

Term                           Coef
Constant                   -177.512
cutting speed (min/sec)  -0.725708
feed rate (mm/rev)          1316.29
axial depth (mm)            118.610
radial depth (mm)           38.8762


Predicted Response for New Design Points Using Model for cutting force (N)

Point      Fit   SE Fit        95% CI              95% PI
```

1	114.694	15.4562	(82.640, 146.748)	(37.015, 192.373)
2	238.823	16.0084	(205.623, 272.022)	(160.664, 316.981)
3	202.037	15.4093	(170.080, 233.994)	(124.398, 279.676)
4	143.980	15.4093	(112.023, 175.937)	(66.341, 221.619)
5	107.194	15.4562	(75.140, 139.248)	(29.515, 184.873)
6	231.323	16.0084	(198.123, 264.522)	(153.164, 309.481)
7	203.027	15.4562	(170.973, 235.081)	(125.348, 280.706)
8	108.185	16.1435	(74.705, 141.664)	(29.907, 186.463)
9	327.156	16.0084	(293.957, 360.355)	(248.997, 405.315)
10	232.313	6.5905	(218.645, 245.981)	(160.248, 304.379)
11	269.099	16.0084	(235.900, 302.299)	(190.941, 347.258)
12	144.971	15.4562	(112.916, 177.025)	(67.291, 222.650)
13	239.813	15.4093	(207.856, 271.770)	(162.174, 317.452)
14	232.313	6.5905	(218.645, 245.981)	(160.248, 304.379)
15	232.313	6.5905	(218.645, 245.981)	(160.248, 304.379)
16	137.471	15.4562	(105.416, 169.525)	(59.791, 215.150)
17	195.527	15.4562	(163.473, 227.581)	(117.848, 273.206)
18	319.656	16.0084	(286.457, 352.855)	(241.497, 397.815)
19	224.813	15.4093	(192.856, 256.770)	(147.174, 302.452)
20	261.599	16.0084	(228.400, 294.799)	(183.441, 339.758)
21	232.313	6.5905	(218.645, 245.981)	(160.248, 304.379)
22	349.933	16.0084	(316.733, 383.132)	(271.774, 428.091)
23	357.433	16.0084	(324.233, 390.632)	(279.274, 435.591)
24	225.804	15.4562	(193.750, 257.858)	(148.125, 303.483)
25	233.304	15.4562	(201.250, 265.358)	(155.625, 310.983)
26	320.647	15.4093	(288.690, 352.604)	(243.008, 398.286)
27	262.590	15.4093	(230.633, 294.547)	(184.951, 340.229)

APPENDIX C

ANOVA result from Minitab for Full Quadratic Model.

```
The analysis was done using coded units.

Estimated Regression Coefficients for cutting force (N)

Term                                     Coef  SE Coef       T      P
Constant                              236.250    19.01  12.428  0.000
cutting speed (min/sec)               -29.028    10.97  -2.645  0.021
feed rate (mm/rev)                     64.333    12.02   5.351  0.000
axial depth (mm)                       59.305    10.97   5.404  0.000
radial depth (mm)                      56.833    12.02   4.727  0.000
cutting speed (min/sec)*               17.416    15.71   1.108  0.289
  cutting speed (min/sec)
feed rate (mm/rev)*                   -17.542    16.28  -1.078  0.302
  feed rate (mm/rev)
axial depth (mm)*axial depth (mm)      -2.167    15.71  -0.138  0.893
radial depth (mm)*radial depth (mm)    -8.375    16.28  -0.514  0.616
cutting speed (min/sec)*                3.332    19.01   0.175  0.864
  feed rate (mm/rev)
cutting speed (min/sec)*               -1.668    19.01  -0.088  0.932
  axial depth (mm)
cutting speed (min/sec)*               -1.250    19.01  -0.066  0.949
  radial depth (mm)
feed rate (mm/rev)*axial depth (mm)    17.500    19.01   0.921  0.375
feed rate (mm/rev)*radial depth (mm)    7.167    24.04   0.298  0.771
axial depth (mm)*radial depth (mm)     20.417    19.01   1.074  0.304

S = 38.02   R-Sq = 88.8%   R-Sq(adj) = 75.7%


Analysis of Variance for cutting force (N)

Source          DF  Seq SS  Adj SS   Adj MS      F      P
Regression      14  137388  137388   9813.4   6.79  0.001
  Linear         4  129123  115574  28893.4  19.99  0.000
  Square         4    5182    4525   1131.2   0.78  0.558
  Interaction    6    3083    3083    513.8   0.36  0.893
Residual Error  12   17345   17345   1445.4
  Lack-of-Fit    9    6576    6576    730.7   0.20  0.973
  Pure Error     3   10769   10769   3589.6
Total           26  154733


Unusual Observations for cutting force (N)

               cutting
                 force
Obs  StdOrder      (N)      Fit  SE Fit  Residual  St Resid
 14        14  325.000  236.250  19.009    88.750      2.70 R
```

R denotes an observation with a large standardized residual.

Estimated Regression Coefficients for cutting force (N) using data in uncoded units

Term	Coef
Constant	182.562
cutting speed (min/sec)	-3.82547
feed rate (mm/rev)	1773.99
axial depth (mm)	-44.0012
radial depth (mm)	11.6913
cutting speed (min/sec)* cutting speed (min/sec)	0.0108850
feed rate (mm/rev)* feed rate (mm/rev)	-7016.80
axial depth (mm)*axial depth (mm)	-8.66600
radial depth (mm)*radial depth (mm)	-3.72200
cutting speed (min/sec)* feed rate (mm/rev)	1.66625
cutting speed (min/sec)* axial depth (mm)	-0.0833750
cutting speed (min/sec)* radial depth (mm)	-0.0208333
feed rate (mm/rev)*axial depth (mm)	700.000
feed rate (mm/rev)*radial depth (mm)	95.5533
axial depth (mm)*radial depth (mm)	27.2233

Predicted Response for New Design Points Using Model for cutting force (N)

Point	Fit	SE Fit	95% CI	95% PI
1	129.988	29.1406	(66.497, 193.480)	(25.619, 234.358)
2	204.070	29.9559	(138.801, 269.338)	(98.610, 309.529)
3	219.555	29.4490	(155.391, 283.719)	(114.776, 324.334)
4	164.834	29.4490	(100.670, 228.998)	(60.055, 269.613)
5	110.404	29.1406	(46.912, 173.895)	(6.034, 214.773)
6	202.820	29.9559	(137.551, 268.088)	(97.360, 308.279)
7	216.237	29.1406	(152.745, 279.729)	(111.868, 320.606)
8	96.334	32.5571	(25.398, 167.270)	(-12.724, 205.392)
9	326.153	29.9559	(260.885, 391.421)	(220.694, 431.612)
10	236.250	19.0092	(194.832, 277.668)	(143.637, 328.863)
11	274.761	29.9559	(209.493, 340.029)	(169.302, 380.220)
12	160.680	29.1406	(97.188, 224.172)	(56.311, 265.049)
13	210.667	29.4490	(146.503, 274.831)	(105.888, 315.446)
14	236.250	19.0092	(194.832, 277.668)	(143.637, 328.863)
15	236.250	19.0092	(194.832, 277.668)	(143.637, 328.863)
16	139.430	29.1406	(75.938, 202.922)	(35.061, 243.799)
17	204.152	29.1406	(140.660, 267.644)	(99.783, 308.521)
18	332.403	29.9559	(267.135, 397.671)	(226.944, 437.862)
19	195.667	29.4490	(131.503, 259.831)	(90.888, 300.446)
20	271.846	29.9559	(206.578, 337.114)	(166.387, 377.305)
21	236.250	19.0092	(194.832, 277.668)	(143.637, 328.863)
22	362.265	29.9559	(296.996, 427.533)	(256.805, 467.724)
23	357.680	29.9559	(292.411, 422.948)	(252.220, 463.139)
24	194.014	29.1406	(130.522, 257.505)	(89.644, 298.383)
25	207.764	29.1406	(144.272, 271.255)	(103.394, 312.133)
26	341.500	29.4490	(277.336, 405.664)	(236.721, 446.279)
27	280.109	29.4490	(215.945, 344.273)	(175.330, 384.888)